TWO-PHOTON UPCONVERSION PROCESS AND ITS APPLICATION TO INFRARED VISION

A Thesis

by

KEYVAN KHOSH ABADY

Submitted to the Graduate and Professional School of
Texas A&M University
in partial fulfillment of the requirements for the degree of

MASTER OF SCIENCE

Chair of Committee,	Peter Rentzepis
Committee Members,	Philip Hemmer
	Alexey Sokolov
	Krishna Narayanan
Head of Department	Costas Georghiades

August 2023

Major Subject: Electrical Engineering

Copyright 2023 Keyvan Khosh Abady

ABSTRACT

This Thesis describes the use of (NaYF4:Yb,Er) microparticles suspended in water and ethanol to convert 980 nm infrared light into 540 nm visible light through a nonlinear stepwise two-photon process. The potential for upconversion enhancement explored by placing IR-reflecting mirrors on four sides of the cuvette containing the microparticles. Additionally, we developed and fabricated microparticle-coated lenses for use as eyeglasses, allowing for the visualization of intense infrared light images converted to visible light. The results of this study have significant implications for the development of new technologies in fields such as infrared vision, optogenetics, imaging, telecommunications, and biomedicine. We also described the design, construction, and results obtained by our novel, compact, and affordable microspectrophotometer capable of accurately recording absorption and emission spectra of microscopic samples.

DEDICATION

To my beloved parents, who have been my constant source of love, support, and inspiration, this thesis is dedicated to you.

ACKNOWLEDGEMENTS

I would like to thank my committee chair, Dr. Peter Rentzepis, and my committee members, Dr. Philip Hemmer, Dr. Krishna Narayanan, and Prof. Alexey Sokolov, for their guidance and support throughout the course of this research.

Thanks also go to my wife for her patience and love.

CONTRIBUTORS AND FUNDING SOURCES

Contributors

This work was supervised by Professor Peter Rentzepis of the Department of Electrical and Computer Engineering.

All the work conducted for this thesis was completed by the student independently.

Funding Sources

This work was supported by the Welch Foundation (under Grant Number 150186) and US Airforce (grant AFGSR #FA9550-18-1-0100).

Its contents are solely the responsibility of the author and do not necessarily represent the official views of the Welch Foundation or US Airforce.

NOMENCLATURE

UCP	Upconverting Particles
ESA	Excited State Absorption
ETU	Energy Transfer Upconversion
CSU	Cooperative Sensitization Upconversion
EMU	Energy Migration Upconversion
PA	Photon Avalanch
FRET	Fluorescence Resonance Energy Transfer

TABLE OF CONTENTS

LIST OF FIGURES

Page

CHAPTER I

INTRODUCTION

Rare earth ions, such as Er^{3+} doped upconverting particles (UCPs), have the unique property of sequentially absorbing two or more low-energy IR photons and emitting a single higher energy, visible photon via a nonlinear stepwise two-photon process[1-3]. In 1959, N. Bloembergen introduced the idea of sensitized triplet-triplet annihilation, where an excited sensitizer molecule transfers its energy to a nearby acceptor molecule, leading to the emission of a higher-energy photon [4]. This groundbreaking discovery paved the way for the development of an efficient method for detecting infrared (IR) photons by leveraging the interaction between IR photons and rare earth (RE) ions embedded in crystalline materials. Due to the development of lasers, François Auzel was able to observe photon upconversion phenomena experimentally in 1966. Furthermore, Auzel suggested that energy transfers between rare earth (RE) ions could occur between two ions, with both being in an excited state during the initial step of energy transfer. This insight challenged the prevailing assumption that energy transfers only occurred from an excited state ion to another ion in its ground state [5].

Upconversion process finds application in various fields, including super-resolution microscopy [6], enhancing solar cell efficiency [7-9], detection of latent fingerprints [10, 11], optogenetics [12-14], high-resolution bioimaging [15-17], photodynamic therapy [18, 19] and sensing [20, 21]. UCPs are also considered promising alternatives for conventional luminophores such as organic dyes and semiconductor quantum dots [22, 23], because they possess unique optical properties such as a long lifetime of the intermediate energy levels [24-26], high

photostability [2, 27], low chemical toxicity [28], multiple-peak spectral patterns [2], lack of photo-blinking even at the millisecond and second-time scales [29], and absence of photobleaching even after hours of continuous excitation [30, 31]. In addition, the scattering of the near-infrared excitation light in many dispersing media such as air, water and biomedical tissues is significantly reduced in comparison to UV and visible light scattering [32-34], which makes it highly suitable for many applications, including aerospace and biomedicine [7, 30, 35].

A photon upconversion process involving lanthanide-doped nanomaterials typically occurs in three steps: stepwise two photon absorption, energy transfer and the emission of photons [36]. Throughout this study, we will explore the concepts of the two-photon absorption and different upconversion energy transfer mechanisms. Then we provide insights into their potential applications in science and technology. We will also discuss the limitations associated with this concept and propose different strategies to overcome them. Furthermore, we will present our novel approach to enhancing upconversion luminescent efficiency by a factor of three. Using this technique, we have developed innovative infrared vision glasses capable of enabling infrared vision in human eyes.

Two photon absorption

The second law of photochemistry states that for each photon absorbed by a collection of molecules, only one molecule is activated for an excited-state reaction assuming a linear response to the incident electromagnetic field [37] . The law is applicable to a variety of photophysical and photochemical processes under conventional continuous wave (CW) light stimulation [38]. In nonlinear optics, the response of the material to light becomes dependent on the intensity or power of the incident light, leading to various nonlinear optical effects [39, 40].

One of the most important phenomena in nonlinear optics is the two-photon absorption process by which a molecule or material absorbs a pair of photons, the sum of whose energy equals the transition energy [41]. This phenomenon can be divided into two categories: simultaneous and stepwise processes.

a) Simultaneous two photon absorption

Simultaneous two photon absorption occurs when a molecule or material absorbs two photons simultaneously, resulting in an electronic transition to a higher energy state via a virtual state. The simultaneous two photon absorption can produce the excited state with lower energy photons than the energy level of the excited state and the probability for the excitation depends on the square of the light intensity. In this process, the combined energy of the two photons must match the energy gap between the initial and final states of the molecule or material. Simultaneous two-photon absorption occurs when the intensity of the incident light is high enough to enable the simultaneous absorption of two photons, leading to a nonlinear response.

The concept of simultaneous two-photon absorption was first described by Maria Goeppert-Mayer in 1931 [42, 43]. This process involves the absorption of an additional photon during the interaction of the first photon with the matter, typically within a very short timescale of approximately 1-2 femtoseconds [44] and thus the probability of occurrence of simultaneous two photon absorption is extremely low ($\sigma = \sim 10^{-54}\, cm^4.s/photon$). As a result, the use of high-power light sources, such as femtosecond and nanosecond pulse lasers, becomes necessary to induce simultaneous two photon absorption which means that the realization of two-photon excitation luminescence needs extremely high excitation energy to ensure a large number of excited photons [45]. This requirement arises due to the fact that the

virtual state involved in simultaneous two photon absorption is not a stationary electronic state. However, during the time when Goeppert-Mayer proposed the concept, these high-power light sources were not yet available.

In 1961, simultaneous two-photon absorption was successfully demonstrated experimentally, a major advancement largely due to the invention of femtosecond pulse lasers. These ultrafast lasers deliver pulses with extremely short durations, typically in the femtosecond (10^{-15} seconds) range, enabling the realization of luminescence signals resulting from two-photon absorption processes [38, 45].

It should be noted that the focus of this study does not include the investigation or analysis of simultaneous two-photon absorption as the main focus of the study. Instead, the focus will be on the stepwise two photon absorption.

b) Stepwise two photon absorption

Stepwise two-photon absorption is a process in nonlinear optics where a molecule or material undergoes a sequential absorption of two photons to transition from the initial state to an excited state. In 1961, Kaiser and Garrett successfully demonstrated two photon absorption in dye solutions using a pulsed ruby laser. This experimental proof laid the foundation for further investigations into two photon absorption [46].

Unlike simultaneous two photon absorption (which involves the absorption of two photons simultaneously) stepwise two photon absorption occurs in two distinct steps. In the first step, the molecule or material absorbs one photon, leading to an intermediate stationary electronic state. Subsequently, in the second step, another photon is absorbed, facilitating the

transition to the final excited state. This sequential absorption of photons allows for the excitation of the system to higher energy levels.

The cross section of stepwise two-photon absorption is a measure of the probability of this process occurring. It is directly proportional to the power intensity of the light source. The higher the power intensity, the higher the probability of stepwise two-photon absorption occurring. This process occurs via an actual stationary electronic state such as an excited state and the power threshold required to induce this process is greatly influenced by the lifetime of the intermediate transient state. Therefore, the probability of the stepwise two photon absorption depends on the lifetime of the intermediate transient state. This means that if the intermediate transient state has a long enough lifetime, the power threshold required to induce stepwise two-photon absorption is greatly reduced. As a result, even continuous wave light sources and sunlight, can induce stepwise two-photon absorption [44].

Energy transfer mechanisms

In the context of energy transfer mechanisms in upconversion processes, the singlet excited state (S1), triplet excited state (T1), and ground state of a photoproduct may all play crucial roles. These states collectively contribute to the intricate energy transfer mechanisms that drive upconversion phenomena, allowing for the efficient conversion of photons and the emission of higher-energy photons. The lifetimes of the S1 states typically fall within the nanosecond time scale, while the lifetimes of T1 states are significantly longer, ranging from microseconds to tens of microseconds.

This significant difference in lifetimes is due to the spin selection rule which dictates the allowed transitions between electronic states based on the spin properties of the involved

particles. The longer lifetimes of T1 states make them more favorable for absorbing another photon, resulting in a lower power threshold for stepwise two-photon absorption compared to the S1 state [38, 44, 47].

The excited states S1 and T1, along with the ground state, are involved in the five types of energy transfer mechanisms observed in upconversion processes, which exhibit high energy transfer efficiency. These mechanisms include: (a) excited-state absorption (ESA), (b) energy transfer upconversion (ETU), (c) cooperative sensitization upconversion (CSU), (d) cross relaxation (CR), and (e) photon avalanche (PA) [48, 49]. These diverse energy transfer mechanisms contribute to the efficient conversion of lower-energy photons into higher-energy ones, enabling various applications in science and technology. In addition to the efficient energy transfer mechanisms discussed in this study, it should be noted that there may be other mechanisms of energy transfer in upconverting particles. These mechanisms have not been explored extensively or found to be efficient up to now. These less efficient processes might involve alternative pathways or interactions that have not been thoroughly investigated in the context of upconverting particles. Additional energy transfer mechanisms may be revealed through further research and exploration of upconversion materials and particles, revealing their potential applications in future upconversion technologies. The five basic efficient energy transfer mechanisms are discussed below [8, 41, 48, 50, 51].

a) Excited state absorption (ESA)

In Excited-state absorption (ESA) process as illustrated in Figure 1, the upconverting material sequentially absorbs one or more low-energy photons and promotes them to a higher energy level or excited state causing the intermediate state to populate. While the low energy

photons are in an excited state, the ion will absorb another low-energy pump photon leading to an even higher excited energy level. This is primarily due to the long lifetime of the intermediate state, allowing sufficient time for the absorption of the second pump photon before the ion decays back to the ground state. Therefore, for this process to occur, the absorption cross-section of the excited ion in the intermediate state should be sufficient to effectively absorb the second pump photon, enabling the ion to reach the higher energy level before returning to the ground state. After the successive absorption of multiple low-energy photons and the promotion of the ion to a higher excited energy level, subsequent emission occurs. The emission process involves the relaxation of the ion from the higher energy level back to the ground state or a lower energy level. During this relaxation, the excess energy acquired from the absorbed photons is released in the form of emitted photons. The emitted photons typically have higher energy than the absorbed photons, resulting in upconversion of the light. The specific emission wavelengths and pathways depend on the energy level structure and transitions within the upconverting material. As a result, upconverting particles can convert lower energy photons, such as infrared light, into higher energy photons, such as visible or ultraviolet light.

In the Excited-state absorption (ESA) process, it is generally preferred to have a low concentration of activator dopants in the upconverting material. This is because high doping concentrations can lead to the degradation of upconversion emission through nonradiative relaxation processes. When the concentration of activator dopants is high, the distance between neighboring ions becomes smaller, increasing the probability of ion interactions with each other such as energy transfer or quenching. These interactions can cause the energy absorbed by one ion to be transferred to another nearby ion without emitting a photon, resulting in energy losses

through nonradiative pathways and the loss of upconverted light emission which reduces the efficiency of upconversion emission.

By keeping the doping concentration low, the distance between activator ions is increased and the interactions between activator ions are minimized which results in reducing the occurrence of nonradiative processes and enhancing the efficiency of upconversion. Therefore, controlling the concentration of activator dopants at low levels is crucial to optimize the upconversion performance of the material.

It is worth mentioning that the efficiency of the Excited-state absorption (ESA) process is significantly reduced due to the weak absorption induced by parity-forbidden 4f-4f transitions within the rare-earth (RE) ions [50]. The low absorption probability hinders the population of the higher excited energy levels, limiting the effectiveness of the ESA mechanism. To mitigate this limitation and enhance the efficiency of ESA-based processes, researchers employ various strategies. These include using sensitizers or co-dopants that can absorb photons efficiently and transfer the energy to the RE ions, selecting host materials that can modify the local electric field and improve the absorption probability, and employing advanced nanostructured designs to enhance light-matter interactions.

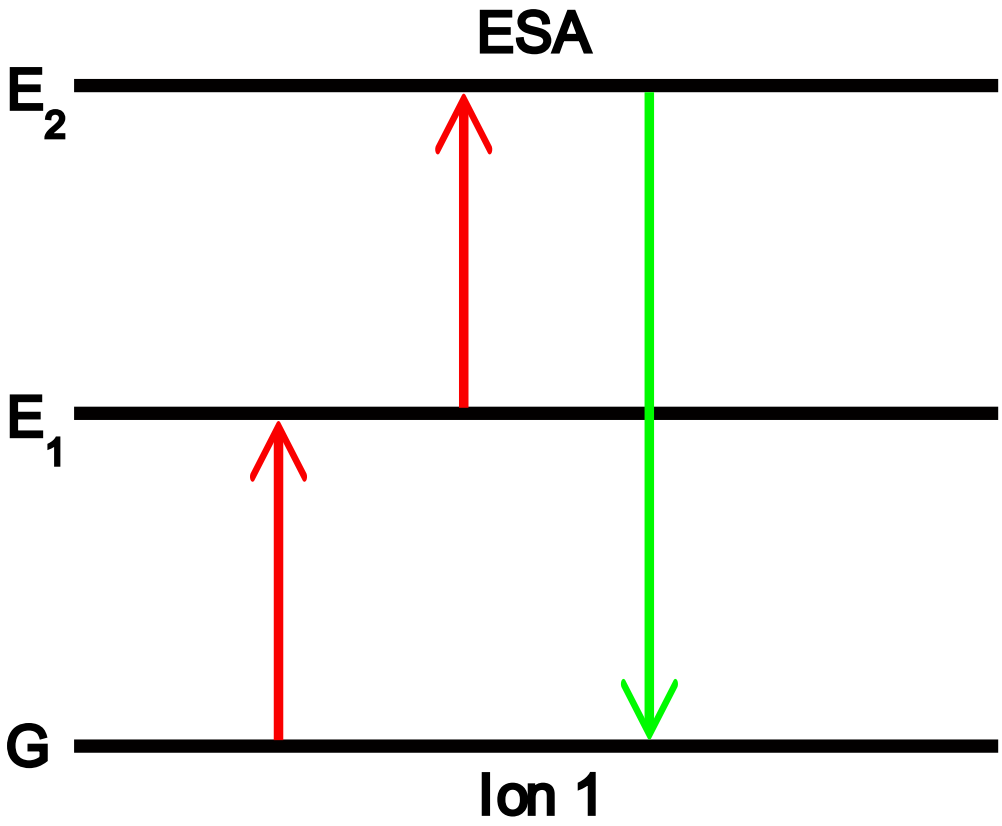

Figure 1- Excited State Absorption (ESA) process for lanthanide doped upconverting particles.

b) Energy Transfer Upconversion (ETU)

In the ETU process as Illustrated in Figure 2, the upconverting material consists of sensitizer ions that absorb the low-energy photons and transfer their energy to activator ions. The sensitizer ions are typically excited to a higher energy level, known as the sensitizer excited state. From this excited state, the sensitizer ions can transfer their energy to adjacent activator ions through a nonradiative energy transfer process. This energy transfer can occur through mechanisms such as dipole-dipole interactions, Förster resonance energy transfer (FRET), or electron exchange interactions. Once the energy is transferred to the activator ions, they undergo a radiative transition to emit a higher-energy photon. This emission occurs at a wavelength shorter than the individual absorbed photons, resulting in an upconversion effect.

The efficiency of the ETU process relies on the efficient energy transfer between the sensitizer and activator ions. Additionally, factors such as the proximity and concentration of the sensitizer and activator ions within the host material, their energy level alignment and coupling strength between them, as well as excitation intensity and the environmental conditions can influence the efficiency of the ETU process.

The ETU process is typically two orders of magnitude more efficient than ESA mainly due to the fact that ESA occurs within a single excited ion, while ETU involves energy transfer between sensitizer and activator ions. Therefore, the resonant absorption energy will achieve more easier in ETU and the excitation lifetime is longer to achieve more efficient upconversion of energy [52].

Most effective upconversion particles to date, including those used in this study, consist of a combination of two ions. These ion pairs are usually Yb^{3+}/Tm^{3+}, Yb^{3+}/Er^{3+}, or Yb^{3+}/Ho^{3+} which help the UCPs absorb light better at around 975 nm, which has reduced scattering compared to UV and visible light.

In this study, we used the well-known upconverting particles which consist of Sodium Yttrium tetra Fluoride ($NaYF_4$) crystalline host matrix doped with Erbium (Er^{3+}) and Ytterbium (Yb^{3+}) lanthanide ions. The Er^{3+} ions act as activators, while the Yb^{3+} ions are the sensitizers. Upon excitation with a 980 nm laser light, a two-photon stepwise process with the ETU mechanism is initiated, resulting in the absorption of 980 nm light and the transition from $^2F_{7/2}$ to $^2F_{5/2}$ state in the Yb^{3+} ion as shown in the energy diagram in Figure 3 and after a two-photon stepwise absorption, 540 nm green light is emitted. Then, this energy will transfer to the neighboring Er^{3+} activator ion through a nonradiative energy transfer process, promoting it to the $^4I_{11/2}$ state. From the $^4I_{11/2}$ state, the Er^{3+} ion can undergo two different pathways: In the

first pathway, the Er^{3+} ion undergoes a non-radiative relaxation process, returning to the $^4I_{13/2}$ state. From there, the second energy transfer occurs, promoting the Er^{3+} ion to the $^4F_{9/2}$ state. In the second pathway, the second energy transfer directly promotes the Er^{3+} ion from the $^4I_{11/2}$ state to the $^4F_{7/2}$ state. From the $^4F_{7/2}$ state, the Er^{3+} ion non-radiatively relaxes to the $^2H_{11/2}$ and $^4S_{3/2}$ states. Finally, from these excited states ($^4F_{9/2}$, $^2H_{11/2}$ and $^4S_{3/2}$), the Er^{3+} ion radiatively relaxes back down to the $^4I_{15/2}$ state, releasing 532 nm high-energy photons. [49, 53]

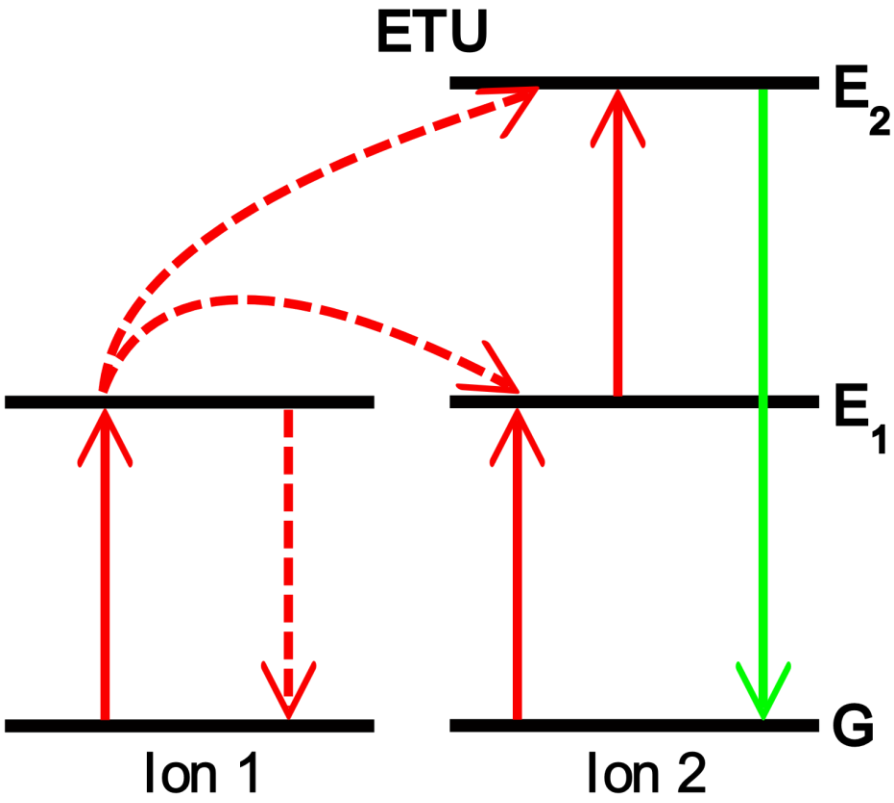

Figure 2- Energy Transfer Upconversion (ETU) process for lanthanide doped upconverting particles.

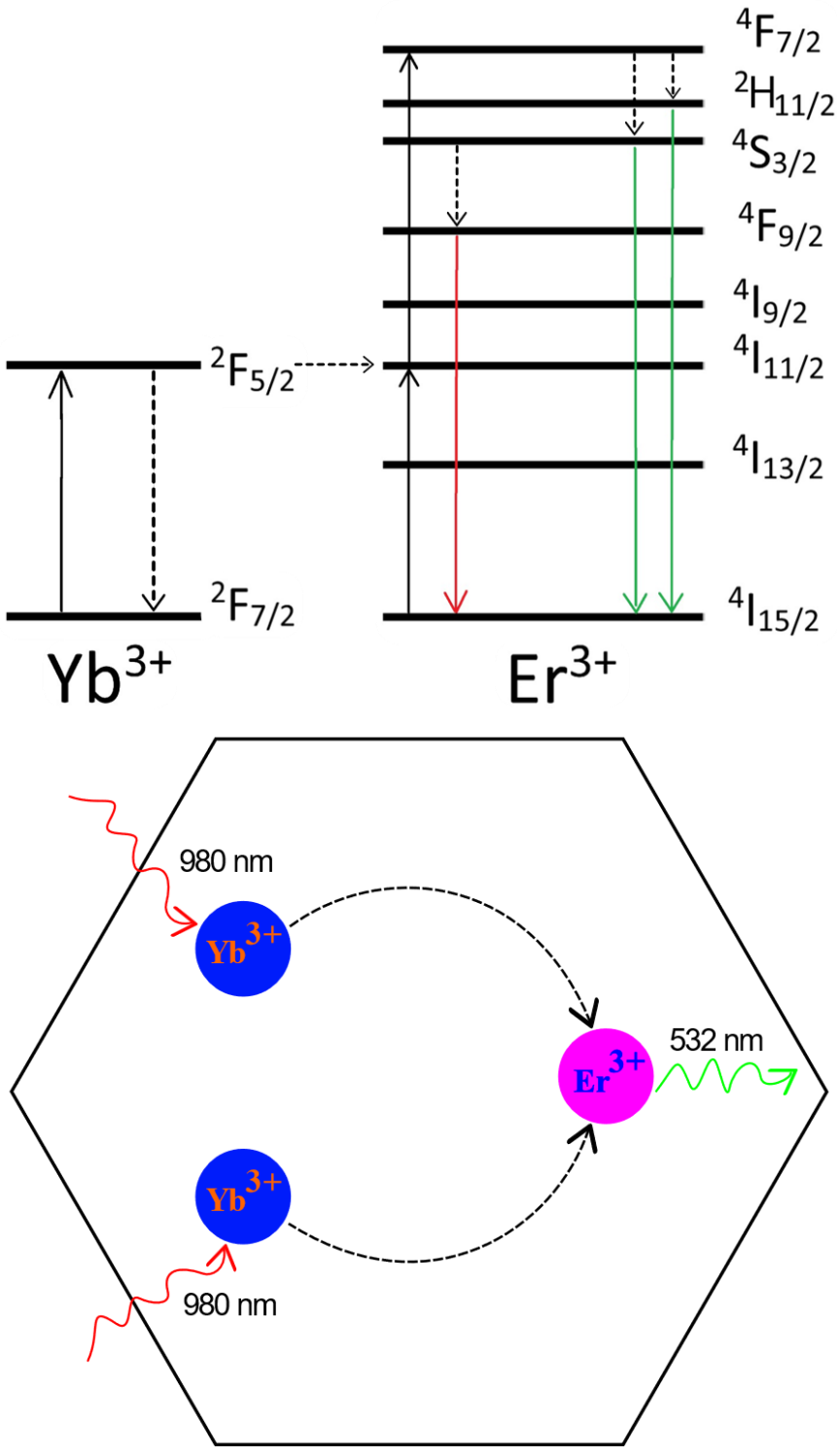

Figure 3- The energy transfer upconversion mechanism in NaYF4:Yb, Er microparticles.

c) Cooperative Sensitization Upconversion (CSU)

Cooperative Sensitization Upconversion (CSU) is a process that involves the cooperation of two or more sensitizer ions to achieve upconversion of energy in a material. In ETU, a single sensitizer ion absorbs a low-energy photon and transfers its energy to an activator ion, which then emits a higher-energy photon. However, in CSU, instead of relying on a single sensitizer ion, multiple sensitizer ions work together to transfer lower energy photons to the activator ions, leading to the emission of a higher energy photon. In this process, multiple sensitizer ions absorb a low-energy photon and get excited to a higher energy state. The neighboring sensitizer ions then transfer their energy simultaneously to the activator ion and excite activator ion to a higher energy level. Finally, the activator ion undergoes a relaxation to its ground state, emitting a higher-energy photon through its radiative transition. The CSU mechanism is illustrated in Figure 4.

Cooperative Sensitization Upconversion (CSU) typically exhibits lower upconversion efficiency compared to ETU and ESA processes owing to the fact that in the CSU process there exists no real intermediate energy level with a long lifetime in the activator [54]. Different ion pairs have been reported to exhibit the cooperative sensitization upconversion mechanism, including Yb^{3+}/Tb^{3+}, Yb^{3+}/Eu^{3+} and Yb^{3+}/Pr^{3+}[55-57].

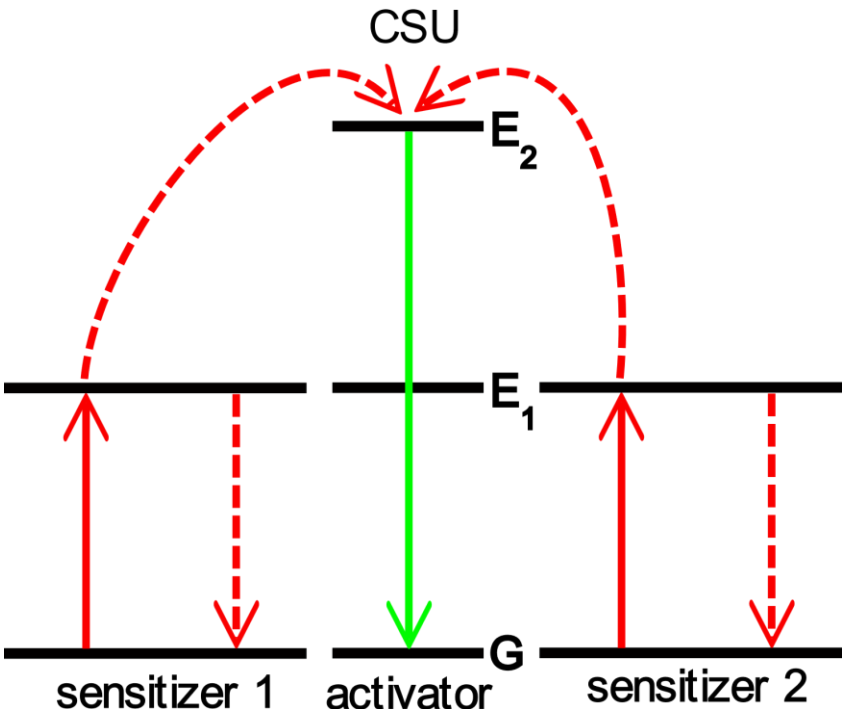

Figure 4- Cooperative Sensitization Upconversion (CSU) process for lanthanide doped upconverting particles.

d) Photon Avalanche

Photon avalanche upconversion is a process in which a single low-energy photon triggers a cascade of energy transfer steps, resulting in the emission of multiple high-energy photons. This process starts with the ground state (state number 1) non-resonant absorption of low-energy photons by upconverting material promoting the material to the intermediate excited state (state number 2). Then the material absorbs another low-energy photon through an ESA process and promotes to the super excited state (state number 3). Subsequently, this ion undergoes a cross-relaxation energy transfer process, where it relaxes back to state 2 while simultaneously promoting a neighboring ion to state 2. This energy transfer cycle continues until the ions in the intermediate excited state exponentially populated above the excitation threshold. As the population of ions in the intermediate excited state grows, a critical point is reached where the

number of superexcited ions surpasses the number of ions in the ground state. In this mechanism, the number of avalanche transitions goes on increasing until the consumption of so excited ions is less than the ground state ions. The photon avalanche mechanism is illustrated in Figure 5.

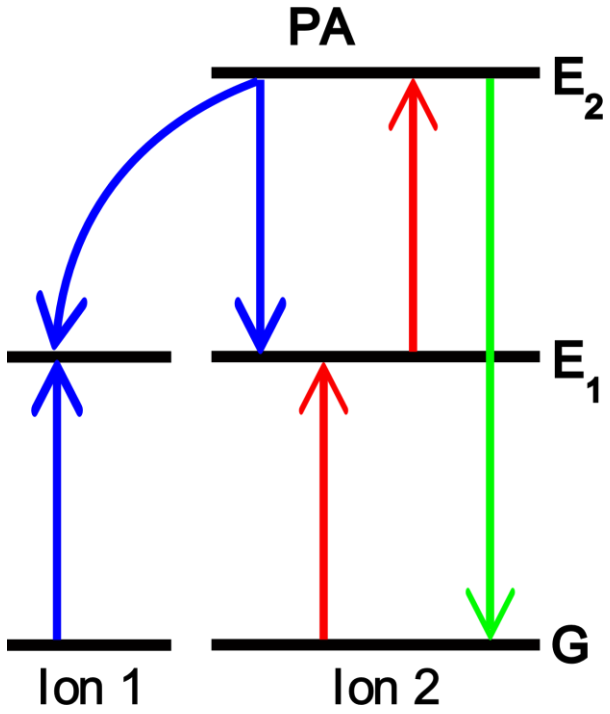

Figure 5- Photon Avalanche (PA) process for lanthanide doped upconverting particles.

e) Energy Migration Upconversion (EMU)

In the EMU (Energy Migration Upconversion) process, shown in Figure 6, luminescent centers are organized into separate layers, including a sensitizer, accumulator, migrator, and activator. When stimulated by low-energy photons, an energy transfer upconversion (ETU) process takes place. The sensitizer first absorbs the photons and transfers the energy to the accumulator, which reaches a higher excited state. To effectively transfer energy, the accumulator should possess energy levels with longer lifetimes, allowing it to efficiently capture and store the energy absorbed from the sensitizer. The energy is then transferred to a migrator

within the same region, and subsequently, through the core/shell interface, to a migrator in a neighboring region. Eventually, the migrated energy is captured by an activator, resulting in upconverted (UC) emissions as electrons return to their ground state. Additionally, UC emissions can also arise from the accumulator ions. This sequential energy transfer mechanism enables efficient upconversion of low-energy photons to higher-energy emissions.

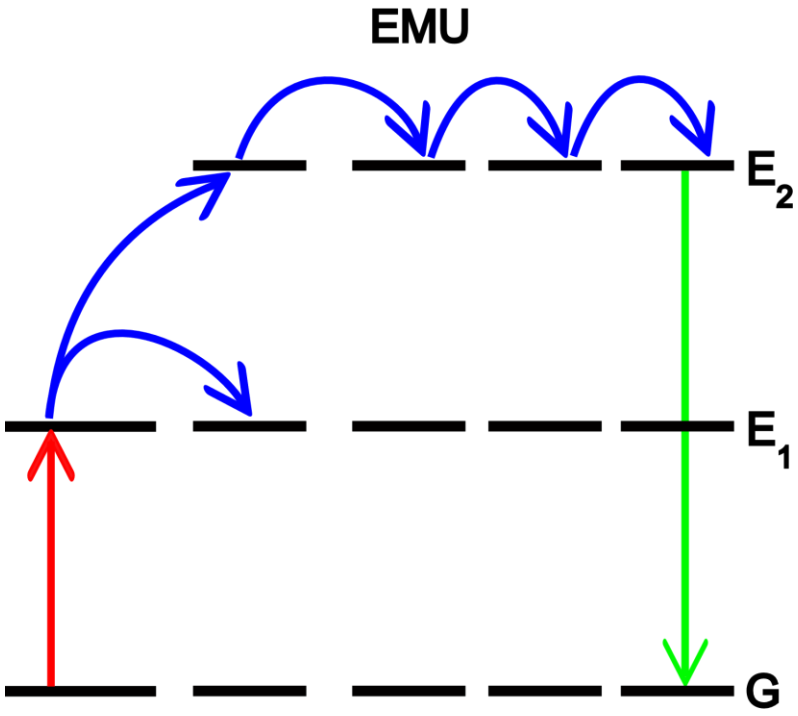

Figure 6- Energy Migration Upconversion (EMU) process for lanthanide doped upconverting particles.

Composition of upconversion materials

Inorganic crystals typically do not demonstrate upconverting (UC) luminescence under ambient conditions. As a result, upconverting particles (UCP) are commonly comprised of a crystalline host with the addition of dopants at low concentrations within the host lattice. These dopants typically exist as localized luminescent centers, and the crystal structure of the host lattice serves as a matrix to precisely position these centers for optimal functionality. Upon excitation, the dopant ion emits radiation as it transitions to a higher energetic state, facilitated by the non-radiative transfer of energy from another dopant ion. The ion responsible for emitting the radiation is known as the activator, while the sensitizer serves as the energy donor [58, 59]. Consideration should be given to the exact manipulation of energy transfer mechanisms within these three components when determining the most appropriate combination of dopant and host. The luminescent behavior of UCP is contingent upon various factors, encompassing the selection of both host and dopant materials, their respective structures and sizes, the concentrations of sensitizers and activators embedded within the host matrix, the power of excitation, and the concentration of UCPs dispersed within the medium. The dopant ions play a critical role in determining the efficiency of photon upconversion. In the context of UCPs, activators, also known as emitters, must possess a substantial number of metastable energy levels. These energy levels need to be far enough apart to stop nonradiative relaxations while still being close enough to make photon absorption and energy transfer in UC processes easier. Numerous suitable host materials doped with transition-metal ions (3d, 4d, and 5d) have been documented for upconversion phenomena. Noteworthy examples include Ti^{2+} [60], Ni^{2+} [61], Mo^{3+} [62], Re^{4+} [63], and Os^{4+}-doped solids [64]. The UC capabilities of actinide-doped materials have also been studied [65].

However, these systems typically exhibit poor optical properties and necessitate low temperatures for operation. In contrast, lanthanide-doped solids display remarkable UC efficiencies, even at room temperature. The lanthanides, which encompass the elements from lanthanum (La) to lutetium (Lu), are characterized by the filling of the 4f-shell. In their most stable oxidation state, they exist as trivalent ions (Ln^{3+}). In the presence of completed $5s^2$ and $5p^6$ subshells, the 4f electrons of Ln^{3+} are effectively shielded, resulting in weak electron-phonon couplings. This unique attribute gives rise to significant phenomena, such as the presence of sharp and narrow f-f transition bands. Moreover, due to Laporte selection rules, f-f transitions in lanthanides are generally forbidden, leading to low transition probabilities and considerably long excited state lifetimes (up to 0.1 s) [5]. Erbium (Er^{3+}), Thulium (Tm^{3+}), and Holmium (Ho^{3+}) are frequently employed as activators, owing to their ladder-like arrangement of energy levels and long excited state lifetimes. For instance, in Er^{3+}, the energy difference ($\sim$10 350 cm^{-1}) between the $^4I_{11/2}$ and $^4I_{15/2}$ energy levels is comparable to that ($\sim$10 370 cm^{-1}) between the $^4F_{7/2}$ and $^4I_{11/2}$ levels. This similarity in energy gaps enables the utilization of the $^4I_{15/2}$, $^4I_{11/2}$, and $^4F_{7/2}$ energy levels for generating UC emission through excitation at approximately 980 nm. Instead of being directly excited to the $^4F_{7/2}$ state, the Er^{3+} ion in the $^4I_{11/2}$ state can relax to the $^4I1_{3/2}$ state, followed by excitation to the $^4F_{9/2}$ state facilitated by phonon-assisted energy transfer. Notably, Er^{3+}, Tm^{3+}, and Ho^{3+} exhibit relatively large energy gaps, which effectively minimize nonradiative relaxations. The transition rate of nonradiative relaxations decreases exponentially as the energy gap increases [58, 59].

In a singly doped system, two significant parameters influence UC processes: the distance separating neighboring activator ions and the absorption cross-section of these ions. The absorption band of Er^{3+} for the 4f-4f transition around 980 nm exhibits weak ground state

absorption, resulting in low pump efficiency. One possible approach to enhance absorption is by increasing the concentration of lanthanide dopants in the material. However, high doping levels can give rise to detrimental cross-relaxation effects, leading to the quenching of excitation energy. To mitigate the quenching effect, it is crucial to maintain a low and precisely adjusted concentration of activator ions. The upper limit of concentration is determined by the specific distance between lattice sites occupied by lanthanide ions. However, in the majority of UC materials, the concentration of Er^{3+} does not exceed 3%. Nevertheless, at these concentrations, the absorption of light is insufficient, which poses a practical limitation on the utilization of these materials as UCPs [59].

As a result, the overall upconversion efficiency for singly doped systems remains relatively low. In order to enhance the absorption of lanthanide-doped phosphors, it is common practice to introduce a sensitizer with a substantial absorption cross-section in the near-infrared (NIR) region. By co-doping the sensitizer alongside the activator, the efficient ETU process between the sensitizer and activator can be harnessed, thereby maximizing the overall absorption capability [58]. Upon excitation from the ground state to the metastable state, activator ions have a propensity to accept energy from adjacent sensitizers, promoting their excitation to higher energy states. Among the various lanthanide ions, trivalent Ytterbium (Yb^{3+}) emerges as an exceptional choice as a sensitizer. Due to the $^2F_{7/2} \rightarrow {}^2F_{5/2}$ transition, the absorption band of Yb^{3+} that is located around 980 nm has an absorption cross-section of 9.11×10^{-21} cm^{-2} which is relatively large among lanthanide ions [66].

Furthermore, the energy level diagram of Yb^{3+} exclusively encompasses a single excited 4f level, namely $^2F_{5/2}$. Notably, the $^2F_{7/2} \rightarrow {}^2F_{5/2}$ transition of Yb^{3+} harmoniously aligns with numerous f–f transitions of typical UC lanthanide ions such as Er^{3+}, Tm^{3+}, and Ho^{3+}. This

alignment facilitates efficient energy transfer from Yb^{3+} to these ions. For instance, the $^2F_{5/2}$ state of Yb^{3+} effectively overlaps with the $^4I_{11/2}$ state of Er^{3+}, enabling effective Yb-to-Er energy transfer. Usually, sensitizer content is co-doped into the lattice in high concentrations (~20 mol %) while the activator content is relatively low (<2 mol%), minimizing cross-relaxation energy loss. Yb^{3+} is a common sensitizer not only for Er^{3+}, Tm^{3+} systems but also for Ho^{3+} [67], and Pr^{3+} [68] ions.

The selection of the host lattice plays a crucial role in determining the inter-ion distance, spatial arrangement, coordination numbers, and energy transfer efficiencies of the dopant ions. The properties of the host material and its interaction with the dopant ions exert a significant influence on the upconversion process [58]. Optimal host matrices for upconversion applications must possess several key characteristics. Firstly, they should exhibit low-phonon energies to minimize non-radiative losses and maximize radiative emission. Additionally, these host materials should demonstrate chemical and thermal stability to ensure long-term performance. High tolerance towards both sensitizer and activator ions is crucial, as is high transparency to allow for efficient migration of NIR photons within the lattice.

Host materials typically require a close lattice match with the dopant ions. Since trivalent rare earth ions share similar ionic sizes and chemical properties, inorganic compounds containing these ions serve as ideal host materials for upconverting lanthanide dopants. Host lattices incorporating cations such as Na^+, Ca^{2+}, and Y^{3+}, which possess ionic radii closely resembling those of the lanthanide dopant ions, aid in preventing the formation of crystal defects and lattice stress, contributing to improved performance and stability [58]. However, when lanthanide ions are doped into a host matrix, the process is often accompanied by the formation of crystal

defects, such as interstitial anions and cation vacancies, to preserve charge neutrality. Unfortunately, these defects can result in increased multi-phonon relaxation rates between metastable states, consequently diminishing the overall intensity of visible emission [54, 58, 69]. To ensure efficient upconversion and maintain a single crystal phase within the host material, strict control over the dopant concentration is essential. By carefully managing the dopant concentration, it becomes possible to minimize the occurrence of crystal defects and optimize the upconversion process. A wide range of materials have been found to exhibit upconversion, but their actual upconversion efficiency can vary significantly. Common host materials for upconversion include oxides such as ZrO_2, Y_2O_3, and phosphates (e.g., $LuPO_4$, YPO_4), owing to their high chemical stability. However, conventional oxygen-based systems often possess large phonon energies above 500 cm^{-1}, primarily attributed to the stretching vibrations of the host lattice [70].

In addition to oxides, various halide host lattices with rare earth dopants have been extensively investigated for their potential as UCPs [5, 71, 72]. These materials exhibit reduced nonradiative losses, but they are hygroscopic and can suffer from lower chemical stability compared to oxide counterparts [58]. Fluoride materials have emerged as a highly promising class of materials for UCPs due to their ability to fulfill the necessary criteria for efficient host matrices. These materials exhibit low phonon energies, typically around 350 cm^{-1} [73], within their crystal lattice, resulting in significantly prolonged lifetimes of the excited states. This characteristic is crucial for efficient photon upconversion. Among the various fluoride host matrices reported, $NaYF_4$ has demonstrated exceptional effectiveness in converting NIR radiation into visible (VIS) light. One of the most efficient UCPs discovered thus far is $NaYF_4$:Yb^{3+}/Er^{3+}, which was first introduced by Menyuk et al. in 1972 [74]. It is widely

recognized that the crystal structure of UCPs significantly influences their optical properties and upconversion efficiency. The optical properties of these materials, such as phase-dependent behavior, can be directly attributed to the distinct crystal fields surrounding trivalent lanthanide ions in matrices with different symmetries. In low-symmetry hosts, the crystal field exhibits more uneven components around the dopant ions compared to counterparts with high symmetry. This uneven distribution of components enhances the electronic coupling between the 4f energy levels and higher electronic configurations, consequently increasing the transition probabilities for f-f transitions of the dopant ions [75].

$NaYF_4$ exists in two primary crystal phases: cubic (α) and hexagonal (β). The α-$NaYF_4$ phase is thermodynamically favored and stable at higher temperatures, while the β-$NaYF_4$ phase exhibits greater stability at lower temperatures [76, 77]. However, it has been observed that the upconversion efficiency of α-$NaYF_4$ is significantly lower than that of β-$NaYF_4$ [78, 79]. In fact, the green emission upconversion efficiency in hexagonal-phase $NaYF_4$:Yb^{3+}/Er^{3+} is approximately ten times stronger compared to that in cubic $NaYF_4$:Yb^{3+}/Er^{3+} [80]. It could be shown that the generally high emission intensities of this phosphor originate from the interaction of dopant ions located on two different lattice sites [58]. The size of the particles plays a crucial role in determining the efficiency of upconverting luminescence, as it influences the surface-to-volume ratio [30]. Increasing the size of the host crystal leads to a decrease in the surface quenching effect due to the lower surface-to-volume ratio. This, in turn, prolongs the lifetime of the intermediate quantum energy state and enhances the quantum yield of emitted photons [35]. Conversely, reducing the crystal diameter for a given laser excitation power density results in a significant decrease in the upconverted luminescence of the upconverting particles [23].

Research has shown that at a power density of 20 W/cm^2, micro-sized $NaYF_4$: Yb, Er particles exhibit a quantum efficiency of 10.2%, while nano-sized particles display a lower quantum efficiency of 0.32% [81]. Additionally, the emission of Yb^{3+}, Er^{3+} co-doped phosphors demonstrate saturation only at high excitation densities, with saturation observed at 100 W cm^{-2} for $NaYF_4$:Yb^{3+}, Er^{3+} [82].

Applications

UCPs are considered promising alternatives for conventional luminophores such as organic dyes and semiconductor quantum dots [22, 23], because they possess unique optical properties such as a long lifetime of the intermediate energy levels [24-26], high photostability [2, 27], low chemical toxicity [28], multiple-peak spectral patterns [2], lack of photo-blinking even at the millisecond and second-time scales [29], and absence of photobleaching even after hours of continuous excitation [30, 31]. In addition, the scattering of the near-infrared excitation light in many dispersing media such as air, water and biomedical tissues is significantly reduced in comparison to UV and visible light scattering [32-34], which makes it highly suitable for many applications, including aerospace and biomedicine [7, 30, 35].

Upconversion process finds application in various fields, including super-resolution microscopy [6], enhancing solar cell efficiency [7-9], detection of latent fingerprints [10, 11], optogenetics [12-14], high-resolution bioimaging [15-17], photodynamic therapy [18, 19] and sensing [20, 21]. In this study we briefly review some of these applications.

Enhancing solar cell efficiency

A solar cell, also known as a photovoltaic cell, is an electronic device that converts sunlight into electrical energy. It is made up of semiconductor materials, such as silicon, which absorb photons from the sun and release electrons. These electrons are then collected by metal contacts

on the cell and channeled into an external circuit to power devices or charge batteries. Solar cells are a key component of solar panels, which can be used to generate electricity for homes, businesses, and even entire communities. They are a clean and renewable source of energy that can help reduce our dependence on fossil fuels and combat climate change.

However, the efficiency of a typical solar cell is fairly low. Improving the efficiency of solar cells has been a major focus of research and development in recent years, with significant progress being made in increasing their efficiency. One of the main reasons for the relatively low efficiency of conventional solar cells is their inability to effectively absorb infrared (IR) light, which accounts for a significant portion of the solar spectrum's energy. Infrared light typically ranges from 700 to 2500 nm and constitutes approximately 52% of the total solar energy. The limited absorption of IR light is primarily due to the sizable bandgap of the light-absorbing materials used in conventional solar cells. Solar cells with larger bandgaps, such as amorphous silicon solar cells, have a narrower range of wavelengths that they can effectively absorb. The bandgap of amorphous silicon is approximately 1.75 eV, corresponding to a cutoff wavelength of around 708 nm. This means that amorphous silicon solar cells can absorb light with wavelengths below 708 nm (in the visible and part of the near-infrared range), but they have limited absorption in the longer-wavelength near-infrared region [9].

One solution to overcome the limitation of absorbing only a portion of the solar spectrum in conventional solar cells is to utilize upconversion materials. These materials can convert low-energy, long-wavelength photons (sub-bandgap photons) into higher-energy, above-bandgap photons that can be effectively absorbed by the solar cell [83]. The result is the prevention of energy loss and the expansion of the solar spectrum that can be used. However, one major obstacle is the low upconversion efficiency of currently existing UC materials. By coupling the

solar cell system with a back-reflecting mirror, the overall efficiency of the system can be significantly increased. This study describes a new technique for increasing the interaction of IR light with microparticles and thereby enhancing the intensity of the upconverted visible light by a factor of three. The back-reflecting mirror plays a crucial role in maximizing the utilization of incident light and enhancing the extraction of upconverted light. It helps to redirect the light back into the upconverting material, allowing for multiple interactions and increased chances of upconversion. Moreover, it minimizes the loss of visible light by reflecting it back into the desired direction, maximizing the overall efficiency of the solar cell system.

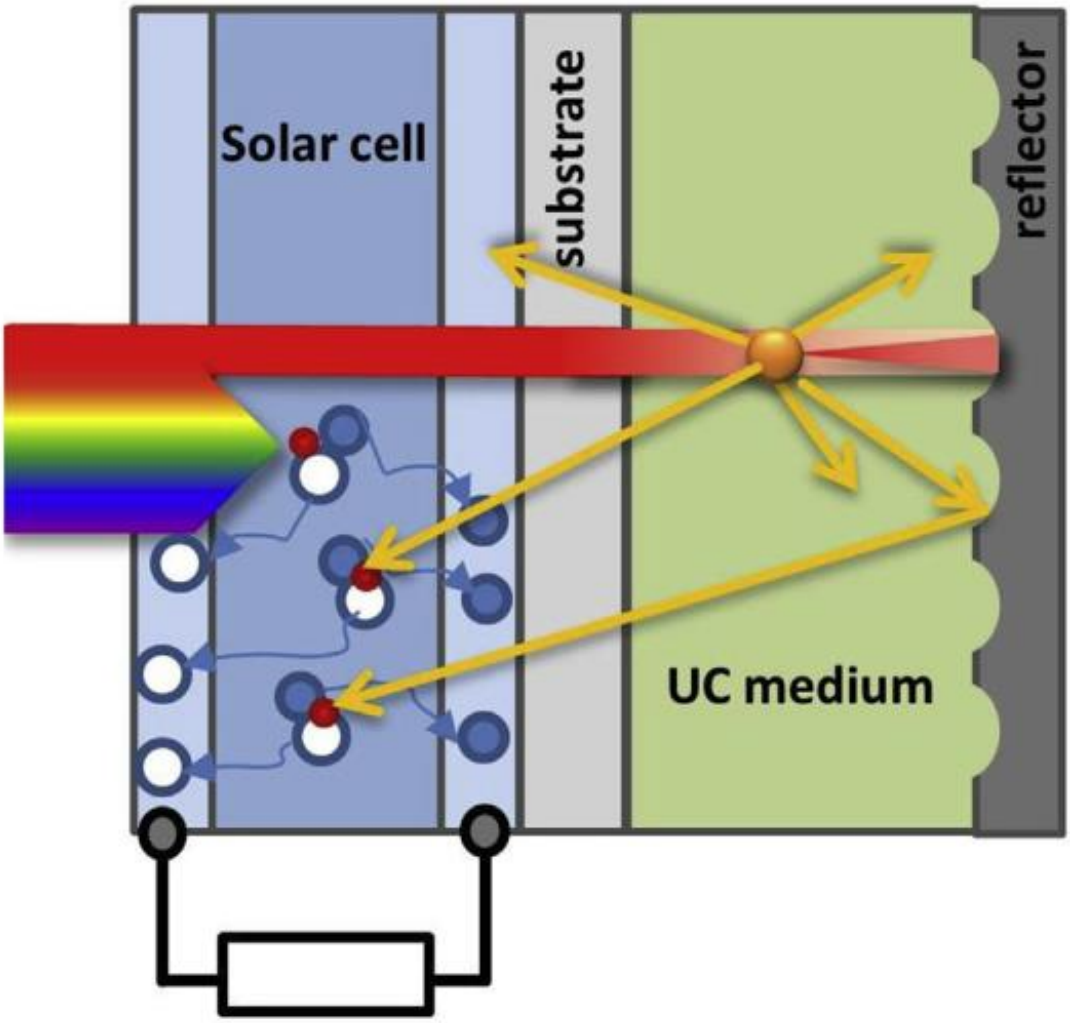

Figure 7- Principle of a solar cell assisted by Upconversion effect. The creation of usable electron-hole pairs in the PV absorber material (left) is augmented by light, usually transmitted unused, which is converted to higher photon energies in the UC unit (right). Reprinted with permission from [84].

Photdynamic therapy

Photodynamic therapy is a medical treatment that utilizes a combination of light and photosensitizing agents to selectively destroy cancer cells or treat certain medical conditions. It is a minimally invasive and targeted approach that is used in the treatment of various cancers, such

as skin cancer, lung cancer, esophageal cancer, and certain types of head and neck cancers. It is also employed in dermatology for the treatment of skin conditions like acne, psoriasis, and precancerous lesions. [85-87]. One advantage of photodynamic therapy is its ability to selectively target affected areas while sparing healthy tissues. This is achieved by controlling the delivery of the photosensitizer and directing the light only to the desired treatment site.

The process of photodynamic therapy involves three key components: a photosensitizer, light of a specific wavelength, and oxygen [88]. The photosensitizer is a light-sensitive chemical compound that is either administered systemically (through injection or oral intake) or applied topically to the targeted area. Once the photosensitizer is absorbed by the target cells or tissues, it remains inactive until it is exposed to light. During the treatment, a specific wavelength of light is applied to the target area, which matches the absorption spectrum of the photosensitizer. This light activates the photosensitizer, causing it to produce reactive oxygen species (ROS) or free radicals. These ROS are highly reactive molecules that can damage nearby cells, including cancer cells or other targeted cells [89]. The ROS generated by the photosensitizer induce a series of biological events, including oxidative stress, inflammation, and cell death. This localized damage to the targeted cells leads to their destruction, shrinking tumors, or resolving certain medical conditions [90].

In the context of photodynamic therapy, upconverting particles can serve as efficient energy mediators. They can absorb near-infrared (NIR) light, which has deeper tissue penetration capabilities, and convert it into visible or ultraviolet (UV) light. This conversion allows for the activation of photosensitizing agents that are typically excited by visible or UV light, even in deep-seated tissues.

The application of upconverting particles in photodynamic therapy offers several advantages. Firstly, the absorption characteristics of biological tissues differ between UV and NIR regions. UV light is absorbed by molecules such as enzymes and nucleic acids present in the tissue, leading to tissue degeneration or damage. In contrast, UCPs can absorb NIR light, which is less likely to be absorbed by these biological molecules. The conversion of NIR light to higher-energy photons occurs in a localized manner within the vicinity of the particles, allowing for precise activation of photosensitizing agents in the target area. This selective absorption by UCPs minimizes the risk of damaging normal tissues during photodynamic therapy [91]. Additionally, the use of NIR light enables deeper tissue penetration, allowing for the treatment of tumors or diseased tissues located at greater depths within the body. This feature is particularly advantageous for treating internal organs or tumors that are not easily accessible [92]. Moreover, upconverting particles offer the possibility of multiplexing, wherein different types of particles can be designed to emit light at distinct wavelengths. This feature enables the simultaneous activation of multiple photosensitizers with different absorption spectra, allowing for combination therapies or targeted treatment of diverse cell populations within the same tissue [93].

It is important to note that while upconverting particles have shown promising results in preclinical studies for photodynamic therapy, further research is still ongoing to optimize their properties, improve their biocompatibility, and enhance their overall therapeutic efficacy. The translation of this technology into clinical practice requires rigorous evaluation of its safety, efficiency, and long-term effects [91].

Sensing

Optical sensing plays a vital role in the field of diagnostics, enabling the detection of minute biochemical entities and molecular targets, as well as the precise monitoring of essential physiological processes. In this context, upconverting particles offer great promise. The ladder-like energy levels these particles further enhance their application for optical sensing. This characteristic enables efficient energy transfer, facilitating sensitive detection when UCPs interact with biomolecular or chemical indicators. The combination of UCPs' frequency conversion capability, their emission properties, and their ability to interface with biomolecular and chemical targets opens up new possibilities for high-sensitivity bio- and chemical-sensing applications. Importantly, this luminescence remains unaffected by biological tissues, making UCPs ideal for applications requiring deep tissue penetration [20].

a) Biomolecules Sensing

The analysis of biomolecules holds significant importance in various fields, including biological detection, genetics, and molecular medicine. UCPs offer distinct advantages, particularly in vitro assays. They serve as luminescent reporters for biomolecule detection, enabling highly sensitive assays with virtually zero background. This unique feature significantly improves the limits of detection (LOD) compared to conventional reporters such as dyes or quantum dots. Recently, Upconversion Fluorescence Resonance Energy Transfer (FRET) based biomolecule sensors have demonstrated high sensitivity in various biological and chemical analyses [20]. In a FRET system, a fluorescence donor and acceptor are conjugated to different biomolecular entities. When the donor and acceptor are in close proximity, the donor fluorescence is effectively quenched by the acceptor. By fixing either the donor or acceptor concentration, the fluorescence intensity becomes linearly related to the target concentration. The FRET-UCPs system has demonstrated low limits of detection (LOD) in various experiments

[94]. In 2011, Saleh et al developed the FRET system employing the acceptor of biotinylated Au nanoparticles and the donor of the avidin-modified $NaYF_4$:Yb/Er NPs in order to detect trace amounts of avidin [95]. The addition of Au-biotin nanoparticles to avidin-conjugated UCNPs results in bonding between the two due to the specific interaction between avidin and biotin. The strong absorption of Au nanoparticles at ~541 nm perfectly matches the UC emission of $NaYF_4$:Yb^{3+}, Er^{3+} nanoparticles. This leads to the quenching of green UC emissions through a FRET process. The linear quenching of green UC emissions enables the detection of trace amounts of avidin proteins [96].

b) Ion Sensing

Several hazardous ions, such as cyanide ions (CN^-) and mercuric ions (Hg^{2+}), have been identified as being extremely toxic to living organisms [97]. Therefore, it is important to detect and evaluate their concentration in order to protect their lives. It has been demonstrated that the luminescent resonance energy transfer (LRET) of lanthanide-doped UCNPs is highly sensitive in living cells [98].

UCNPs are inert to the targeted ions, so they must be used in conjunction with an indicator that is capable of recognizing the ion [99]. UCNPs' fluorescence intensity is modulated by biochemical recognition, enabling precise detection of targeted ions. This detection method allows for accurate measurements of ion concentrations, and colorimetric changes in the solution can be easily observed with the naked eye [98]. Yao et al. developed a highly sensitive and selective CN^- sensor using a chromophoric iridium (III) complex-coated UCNP. The sensor operates based on the LRET mechanism, where the green UC emission is effectively quenched by the chromophoric iridium (III) complex, enabling precise detection of CN^- ions [96]. The addition of CN^- ions results in a significant decrease in the quenching effect, leading to the

ineffectiveness of LRET. Consequently, the green UC emission of the nanoparticles is restored. The UC emission peaks at 540 nm and 650 nm, while the absorbance spectrum of the Ir1 dye exhibits a strong peak at 530 nm, which does not interfere with the red emission band of UCNPs. In the absence of CN^- ions, the chromophoric iridium (III) complex strongly quenches the green UC emission of the UCNPs. However, the absorption of the chromophoric iridium (III) complex at ~500 nm is highly sensitive to CN^- ions, enabling ratiometric evaluation of CN^- concentration by utilizing the green UC at 540 nm and the unaffected red UC at 650 nm.

c) Gas Molecules Sensing

Detecting gas-phase molecules such as oxygen, carbon dioxide, and ammonia at low concentrations has a wide range of industrial, environmental, and biological applications. As a result of their outstanding characteristics, UCNPs have attracted considerable attention for use in gas molecule sensing [99]. A first oxygen sensor based on UCNPs has been presented by the Achatz et al [100]. $NaYF_4$: Yb, Tm UCNPs were utilized in the study, exhibiting dual emission bands in the blue and red regions of the spectrum upon excitation with a 980 nm diode laser (Figure 8A). This unique emission served as an excitation light source for an oxygen probe, which is typically not photo excitable by NIR laser light. To enable oxygen sensing, a cyclometalated iridium (III) complex was selected as the quenchable probe due to its absorption maximum at 468 nm (Figure 8B), which strongly overlaps with the two shortwave emissions (at 455 and 475 nm) of the UCNPs. The luminescence of the iridium complex in the green to yellow range (Figure 8C) peaks at 568 nm, is highly sensitive to oxygen quenching and exhibits minimal overlap with the red emission of the UCNPs beyond 630 nm. Consequently, band C can be easily separated from the UCNP emissions using an interference filter.

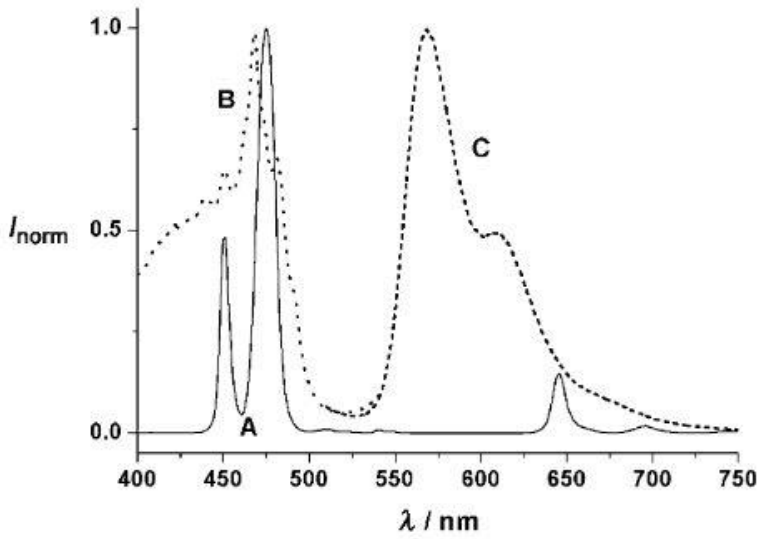

Figure 8- Emission spectra of the NaYF4:Yb,Tm nanoparticles (**A**), the absorption of the oxygen probe (**B**), emission spectrum (**C**). Reprinted with permission from [100].

Infrared Vision

Human eyes can perceive a limited range of wavelengths known as the visible spectrum, which spans from approximately 400 to 750 nanometers (nm). This means that sunlight outside this spectral region, including the ultraviolet (UV) and infrared (IR) regions, is invisible to our eyes. Despite a significant amount of UV and IR radiation reaching the Earth's surface, our eyes lack the natural ability to detect these wavelengths. Infrared vision refers to the ability to perceive and detect infrared (IR) radiation, which is electromagnetic radiation with wavelengths longer than those of visible light. It allows organisms or devices to see and interpret the heat emitted by objects and living beings. By incorporating upconverting particles into imaging devices or eyewear, it becomes possible to visualize and perceive infrared radiation as visible light. The upconverted visible light provides a representation of the infrared scene, allowing individuals to see and interpret objects or scenes that emit IR radiation.

In our earlier studies, we have shown that these upconverting particles can be utilized to induce infrared vision in humans by converting bright infrared light to visible light. However, one major limitation regarding such uses of UCPs is that their upconversion quantum yield is typically less than 1% at room temperature [83, 101] due to the small excitation cross-section of the lanthanide-doped materials (e.g., Nd3+, Ho3+, Er3+, Tm3+, Yb3+)[35, 101-103]. Therefore, enhancing the upconversion luminescence efficiency is one of the major challenges encountered in this field. This study describes a new technique for increasing the interaction of IR light with microparticles and thereby enhancing the intensity of the upconverted visible light by a factor of three. We then used this technique to develop and manufacture thin eyeglass lenses that are coated with upconverting particles (UCPs), enabling the conversion of near-infrared (NIR) images into visible light images at a wavelength of 540 nm. These specially designed lenses allow users to perceive and interpret NIR content in a format that is visible to the human eye. By harnessing the unique properties of UCPs, our eyeglasses provide a practical solution for enhancing vision and expanding the range of detectable wavelengths beyond the limitations of natural human eyesight.

Microphotospectrometer

Microphotospectroscopy is a scientific technique that combines microscopy and spectroscopy to study the properties of materials at a microscopic level. It involves the use of a microscope equipped with a spectrometer to analyze the interaction of light with a sample. In microphotospectroscopy, a focused beam of light is directed onto a small area of a sample, and the resulting interaction between the light and the sample is measured and analyzed. The light can be of various wavelengths, including visible, ultraviolet, and infrared, depending on the specific technique and the properties being investigated.

By examining the interaction of light with the sample, microphotospectroscopy provides valuable information about the composition, structure, and properties of the material. It can reveal details about chemical composition, molecular structure, electronic transitions, and other characteristics that are not easily observable with conventional microscopy alone. Absorption Spectroscopy measures the absorption of light at specific wavelengths, providing information about the sample's composition, concentration, and electronic states. At present, the availability of commercially accessible spectrophotometers capable of measuring the absorption spectrum of microscopic samples is limited. Furthermore, the few options that do exist are often prohibitively expensive. Our design, presented here, reduces that cost by more than ten times. The research presented here describes the design, construction, and means for recording absorption spectrum of the live species, such as the chlorophyl that exist in the Chlamydomonas Reinhardtii live cells that absorb in the visible spectral regime (400 nm - 700 nm). Chlamydomonas reinhardtii is a single-celled green alga that serves as a model organism for studying various biological processes, including photosynthesis, flagellar motility, and cell biology. It belongs to the Chlorophyta division, which includes a diverse group of green algae. Chlamydomonas reinhardtii has a simple cellular structure and is about 10 micrometers in size. It is unicellular, and each cell contains a nucleus, chloroplasts, mitochondria, and a contractile vacuole. The alga is typically found in freshwater environments, such as ponds and lakes, although it can also grow in soil and snow. One of the key characteristics of Chlamydomonas Reinhardtian is its ability to perform photosynthesis. Like plants, it possesses chloroplasts that contain the pigment chlorophyll, allowing it to convert light energy into chemical energy through the process of photosynthesis. This alga has been extensively studied to understand the molecular mechanisms

of photosynthesis, including the structure and function of photosynthetic proteins. Another notable feature of Chlamydomonas Reinhardtian is its two whip-like flagella that protrude from the cell. These flagella are involved in cell motility and allow the alga to move in liquid environments. The study of Chlamydomonas flagella has contributed to our understanding of how flagellar movement is controlled and how it relates to other cellular processes. Due to its relatively simple cellular organization, Chlamydomonas Reinhardtian has been used as a model organism for genetic and molecular studies. Researchers have developed tools and techniques to manipulate its genetic material, allowing the investigation of specific genes and their functions. This alga has contributed significantly to our understanding of fundamental biological processes and has practical applications in biotechnology and biofuel research.

CHAPTER II

MATERIALS AND METHODS

The upconverting particles [$NaY_{0.77}Yb_{0.20}Er_{0.03}F_4$] which are 1-5 microns in size with an average of 2 microns, were purchased from Sigma Aldrich and used as received. The structure of the microparticles was confirmed by XRD. The upconverted luminescence of upconverting particles (UCPs) exhibits a significant increase when the crystal diameter is enlarged, under a constant laser excitation power density. This phenomenon, as discussed in the Introduction part, suggests that larger UCPs have higher efficiency in converting low-energy photons to higher-energy photons. This is the reason that we chose to work with micro-sized particles.

However, the large size of the particles presents a challenge as they have a tendency to settle down, resulting in an inhomogeneous solution of upconverting particles during experiments. To address this issue, a magnetic stirrer was employed to ensure continuous stirring of the solution. This stirring action effectively prevents the microparticles from settling down, maintaining a homogeneous distribution, and facilitating accurate and reliable measurements in the experimental setup.

To maintain a consistent and stable power of the 980 nm excitation light throughout our experiments, we employed a 500 mW/cm2 continuous wave (CW) diode laser as our excitation light source. For power monitoring, we relied on an EPM1000 Molectron optical power meter equipped with a PM3Q sensor. This power meter was utilized continuously to measure the power of the 980 nm laser, ensuring its constancy, and preventing any fluctuations during the course of our experiments.

The intensity of the upconverted 540 nm green light was measured using a Hamamatsu-R928 photomultiplier tube, which was connected to an oscilloscope. The photomultiplier tube is known for its reliable performance in detecting light intensities. Figure 9 provides the typical spectral response exhibited by this specific photomultiplier device.

In all the described experiments, a 1cm glass cuvette with a transmission rate of 85% at both the 980 nm excitation wavelength and the 540 nm upconverted wavelength was employed. This glass cuvette was chosen for its ability to effectively transmit light at these specific wavelengths. Figure 10 provides the transmission spectrum of the glass cuvette, demonstrating its transmission characteristics across different wavelengths.

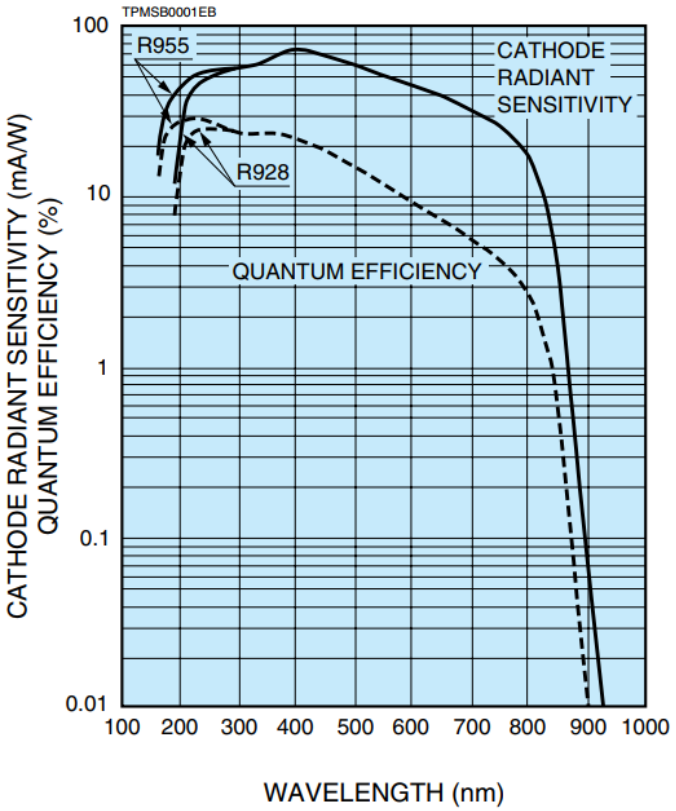

Figure 9- Spectral response of R928 photomultiplier.

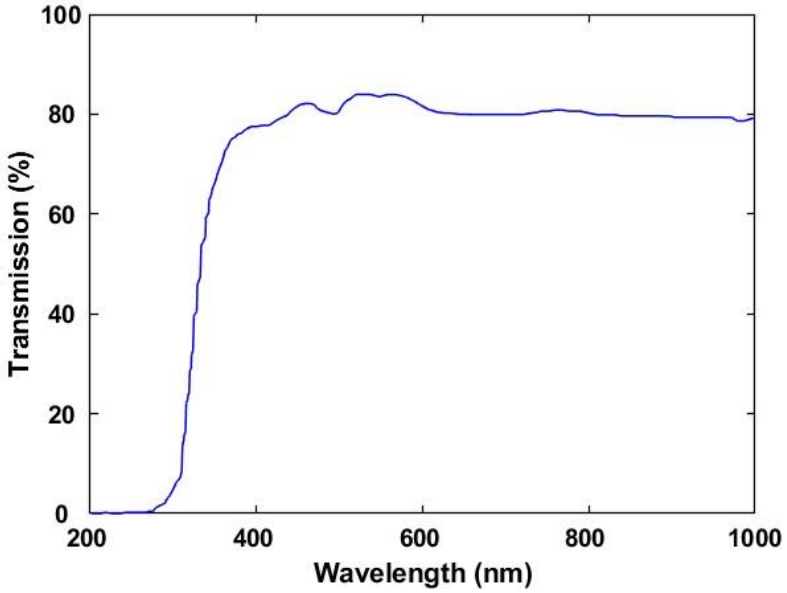

Figure 10- Transmission spectrum of the glass cuvette.

In our study, we utilized mirrors made of glass, measuring 1cm×1cm×1mm in dimensions. These mirrors were coated with Aluminum, which provided a high reflectance of approximately 95% at both the 980nm and 532nm wavelengths. The reflectance spectrum of these mirrors is depicted in Figure 11, illustrating their reflective properties across different wavelengths. To ensure optimal coverage, these mirrors were placed on four sides of the cuvette, covering an area of 1cm×4cm on each side.

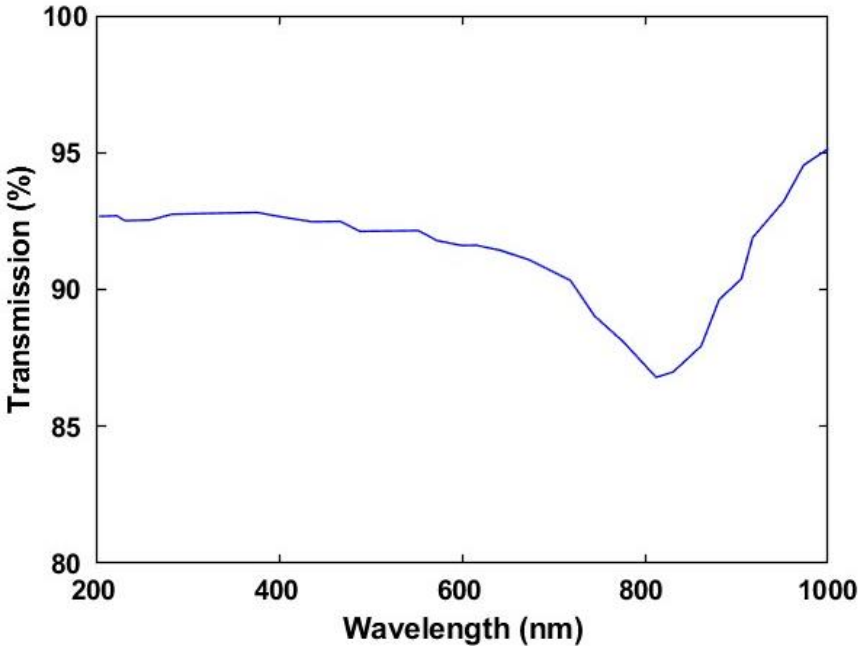

Figure 11- Reflectance of the Aluminum mirrors used.

To fabricate the microparticle coated eye lenses, we followed a specific procedure. First, we prepared a clear solution by combining equal amounts of polyepoxides and hardener. Immediately after, we introduced the upconverting microparticles into the mixture, resulting in a solution with a concentration of 50mg/ml. Subsequently, the mixture underwent a curing process at room temperature for a duration of 48 hours, allowing the materials to solidify and form the desired lenses.

The IR vision lenses were also integrated with specific IR filters that were designed to reflect the 980 nm IR light while allowing the transmission of the 532 nm visible light, as demonstrated in Figure 12, depicting the transmission spectrum of these filters. This specific design was chosen to serve two primary purposes. Firstly, by reflecting the IR light back towards the upconverting particles, they facilitate the generation of additional visible light. Secondly, these filters played a crucial role in protecting the eyes from potential damage by effectively

filtering out harmful IR radiation while allowing safe transmission of visible light. These carefully chosen filters ensure an optimized balance between IR reflection and visible light transmission, enabling enhanced IR vision while prioritizing eye safety.

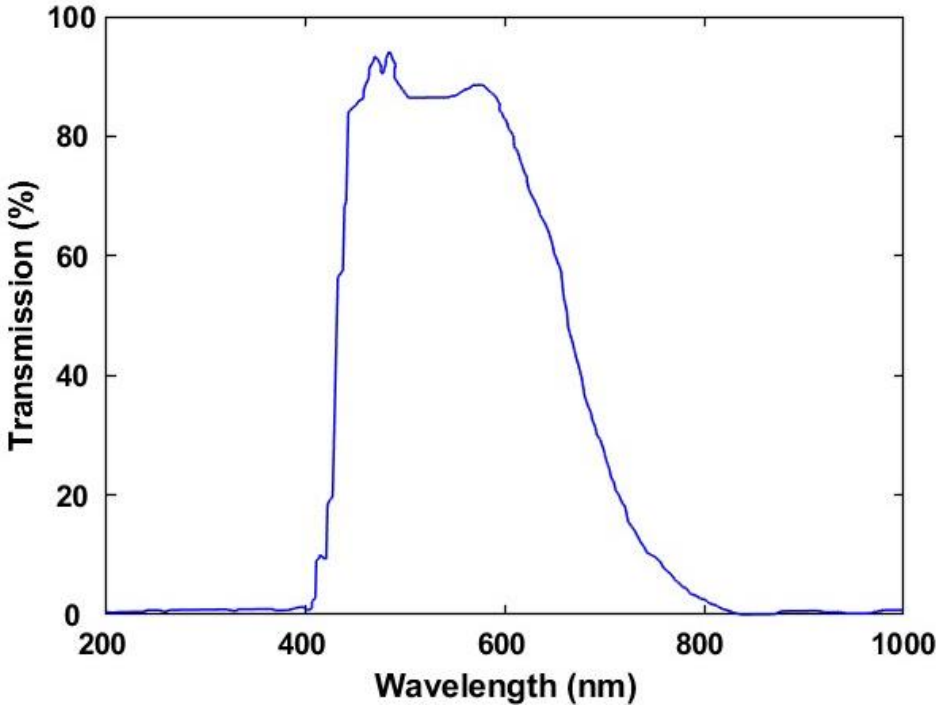

Figure 12- Transmission spectrum of the IR-filter used in our experiments.

To record the emission spectra, we utilized a Shimadzu RF-5301PC spectrofluorophotometer and a USB spectrometer from B&W Tek. For the measurement of absorption spectra, we employed Shimadzu UV-160U and Shimadzu-1201 UV-Vis spectrophotometers. Additionally, the excitation spectra were recorded using a Shimadzu RF5000U spectrofluorophotometer. These spectroscopic instruments were carefully chosen for their precision and reliability in obtaining accurate and detailed spectral data for our study.

The absorption cross-section of the $NaYF_4$:Yb,Er microparticles was determined by:

$$A = -log_{10}\frac{I}{I_0} = C \times \varepsilon \times L \quad \textbf{(1)}$$

where A is the absorbance, I_0 and I are the intensities of the incident and transmitted light, C is the concentration of attenuating species in the solvent, ε is the molar absorption coefficient (Liter×mol^{-1}×cm^{-1}) at the desired wavelength, and L is the optical path length (cm). The molar absorption coefficient was calculated from the ratio of A to C.

Chlamydomonas reinhardtii cells were procured from Carolina Biological, a trusted supplier known for providing high-quality biological materials. The cells were cultured and carefully maintained under optimal growth conditions to ensure their vitality and health throughout the study. To conduct spectroscopic measurements, the harvested Chlamydomonas reinhardtii cells were prepared according to established protocols. This involved taking appropriate steps to ensure the integrity of the cells and their chlorophyll content, which is crucial for accurate absorption spectrum analysis.

The experimental setup of spectrophotometer, employed a standard visible microscope equipped with a comprehensive full spectrum light source. This light source facilitated the illumination of the cells, ensuring that light of various wavelengths was available for absorption by the chlorophyll molecules within the cells. To capture the absorption data, a precise spectrometer was seamlessly integrated with the microscope, enabling precise measurement of the light absorption characteristics. To facilitate accurate targeting and visualization of individual cells, a camera was affixed to the microscope. This allowed researchers to precisely locate and focus on specific cells of interest, ensuring the reliability and specificity of the measurements.

CHAPTER III

RESULTS AND DISCUSSION*

Excitation and emission spectra of $NaYF_4$:Yb,Er UCPs

Figure 13 shows the excitation spectrum of [NaYF4:Yb,Er] when the emission is set at 540 nm. The spectrum reveals a distinct band with a peak centered at 976 nm, indicating the excitation wavelength at which the material exhibits maximum absorption and efficiency for generating the desired emission at 540 nm. By analyzing this excitation spectrum, we gain valuable insights into the optimal excitation conditions for generating the desired emission wavelength. The excitation spectrum of NaYF4:Yb,Er clearly indicates that the material exhibits maximum absorption and efficiency when excited at a wavelength of 976 nm.

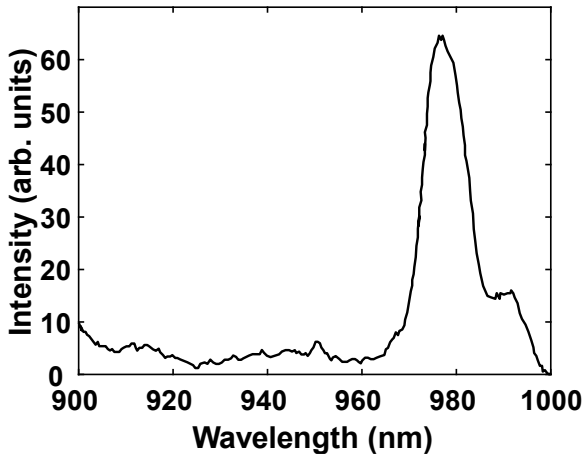

Figure 13- Excitation spectrum of the NaYF4:Yb,Er micro-crystals

The corresponding intense upconverted spectrum obtained from a stepwise two-photon process excitation at 980 nm is illustrated in figure14.

* Part of the data reported in this chapter is reprinted with permission from "*Enhancing the upconversion efficiency of NaYF4:Yb,Er microparticles for infrared vision applications*" by Keyvan Khosh Abady, Dinesh Dhankhar, Arjun Krishnamoorthi and Peter Rentzepis, 2023. *Scientific Reports*, 8408, Pages 1-8, Copyright [2023] by Springer Nature.

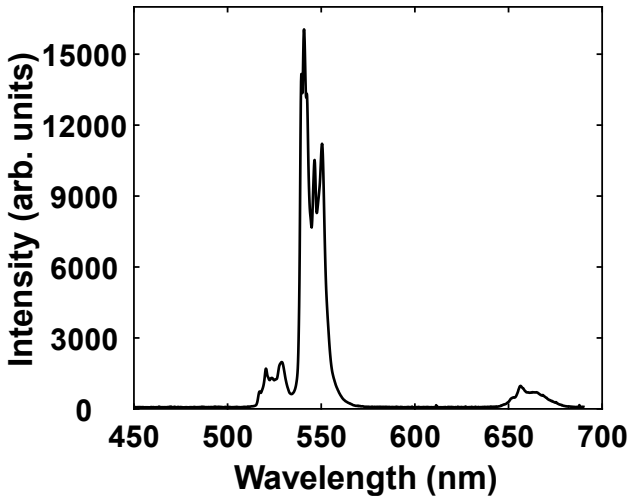

Figure 14- Emission spectrum of the NaYF4:Yb,Er microcrystals under 980nm excitation light

The molar absorption coefficient of NaYF4:Yb,Er dispersed in water at 980 nm was determined to be 150.52 Liter×mol^{-1}×cm^{-1}, obtained from the slope of the linear plot shown in Figure 15. Notably, this molar absorption coefficient value remains independent of the solvent type, as we utilized the same solvent (distilled water) as the reference.

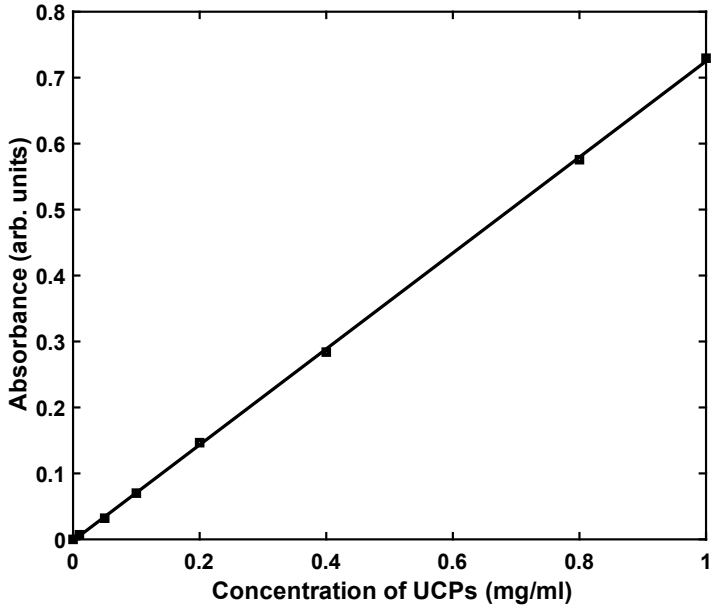

Figure 15- Absorbance of NaYF4:Yb,Er at 980 nm vs. concentration in a water solvent

Applying the Beer-Lambert law to the data shown in Figure 15, we determined that the absorbance depended linearly on the concentration of the UCPs in the solution. As the concentration increased, the absorbance of the 980 nm light in the solution also increased, while the penetration depth decreased. We are investigating whether the dominant mechanism in these values is scattering or absorption in order to determine the accuracy of the calculated extinction coefficient. By enhancing the molar extinction coefficient cross-section, we can effectively increase the efficiency and intensity of the upconverted emission generated by the UCPs.

Effect of the dispersion medium and concentration of UCPs on the intensity of the green upconverted light

Figure 16 illustrates the absorption spectra of water and ethanol at room temperature. It is evident from this figure that water exhibits an absorbance of 0.249 at the 980 nm laser pumping wavelength. This absorbance value indicates that when we excite the sample with 980 nm light, a significant proportion of the excitation light intensity is absorbed by water. Consequently, the intensity of the upconverted 540 nm light is proportionally decreased.

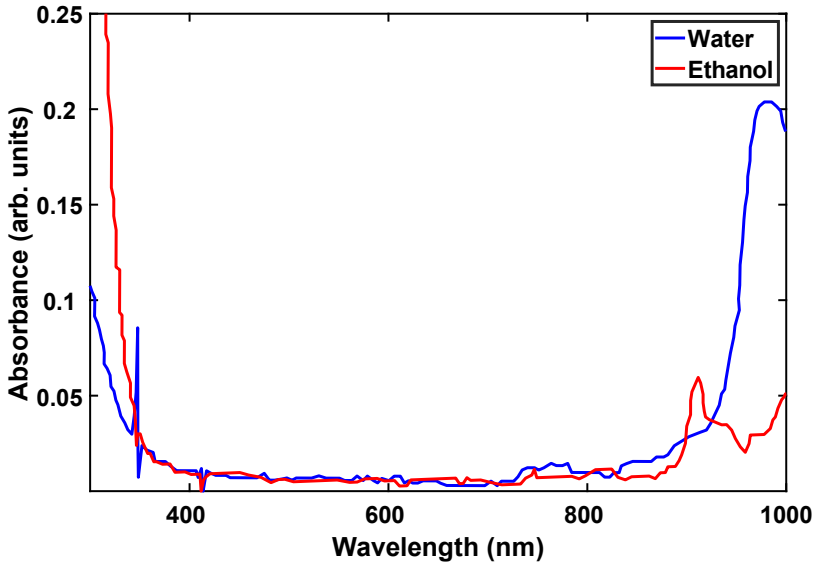

Figure 16- Absorption spectra of water and ethanol measured at room temperature.

In order to mitigate this absorption effect, we conducted the experiment using ethanol as the solvent instead of water. The absorption spectrum of ethanol, as illustrated in Figure 16, demonstrates that its absorbance at 980 nm is only 0.068, significantly lower than the absorbance of water (0.249) at the same wavelength. Based on this observation, we selected ethanol as the solvent for the experiments presented in this study. Utilizing ethanol allows for reduced absorption of the excitation light at 980 nm, enabling a higher proportion of the IR light to contribute to the generation of upconverted light at 540 nm.

Figure 17 displays the relationship between the concentration of upconverting particles dispersed in water and ethanol and the corresponding upconversion emission. For concentrations up to 1 mg/mL, the intensity of the upconverted light exhibits a linear dependency on the concentration. By analyzing the data presented in the figure, it becomes evident that as the concentration of upconverting particles increases, the intensity of the upconverted light proportionally rises, exhibiting a consistent linear trend. This linear relationship suggests that the

upconversion process is directly influenced by the concentration of the particles, allowing for precise control over the emitted light intensity.

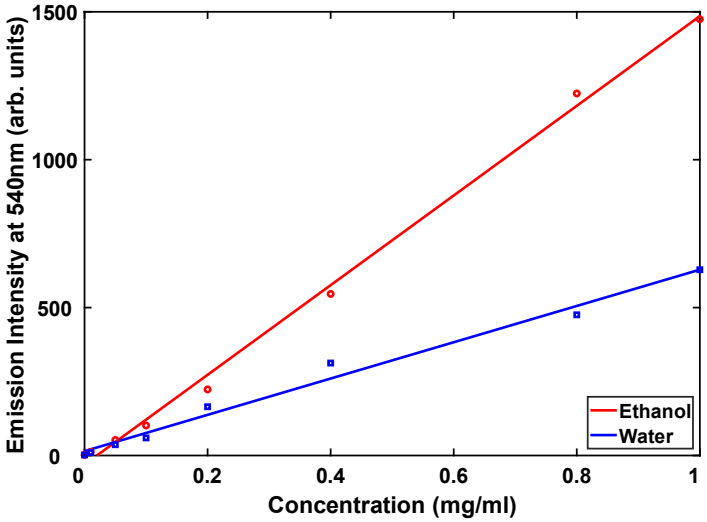

Figure 17- Upconversion emission intensity measured at 540 nm versus concentration of upconverting particles dispersed in ethanol and water.

Effect of the mirror induced multi-reflection on the intensity of the green upconverted light under 980 nm excitation

Only a fraction of the incident infrared light is absorbed by the upconverting particles, while the remaining portion of light is either scattered or transmitted through the sample. To maximize the utilization of the transmitted infrared light, we employed a mirror configuration that reflects this light back into the sample, enabling a second pass through the upconverting particles. In an ideal scenario, a single mirror can lead to a two-fold enhancement in the intensity of the upconverted emission.

To further enhance the upconverted emission intensity and capture the scattered infrared

light from various directions, we placed mirrors on the sides of the cuvette. This arrangement ensures that the scattered infrared light is reflected back into the sample, increasing the chances of interaction with the upconverting particles and improve the efficiency of upconversion processes. By optimizing the use of mirrors in this manner, we can maximize the overall upconverted emission intensity and improve the performance of our experimental setup.

Figure 18 presents the upconverted emission spectra obtained from a suspension of UCP in ethanol with the concentration of 0.1 mg/mL under 980 nm laser excitation, both with and without a single back reflecting mirror. The results clearly show an enhancement of nearly two times when the mirror is used. However, when water was used as the dispersion medium, the upconversion emission intensity and enhancement factor were slightly lower than two. This discrepancy can be attributed to the absorption of a portion of the 980 nm light by water, leading to additional attenuation of the reflected light.

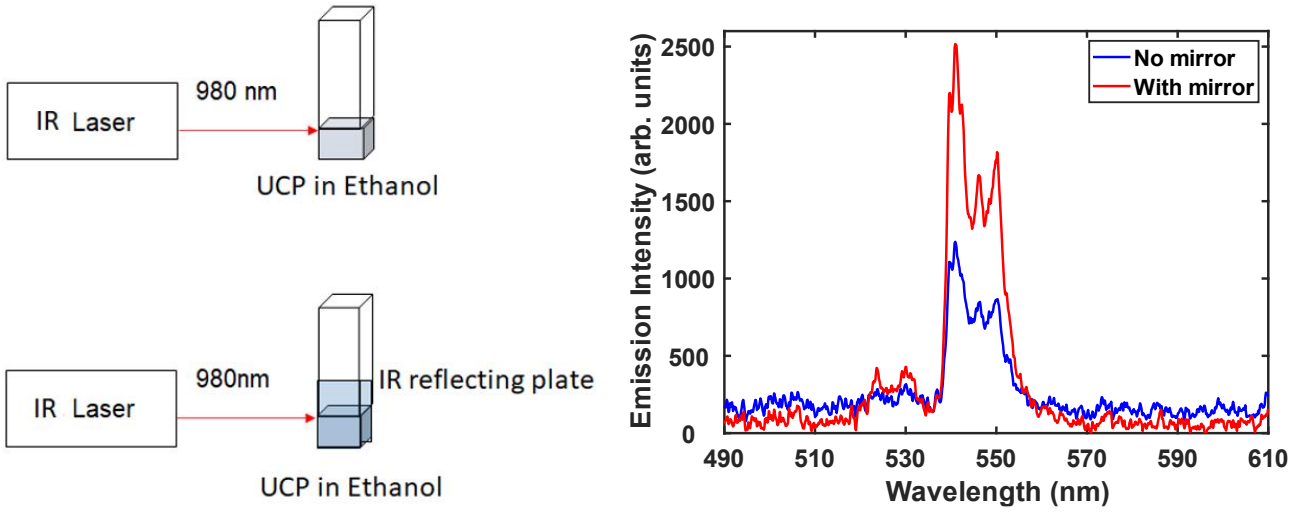

Figure 18- Two times enhancement of upconverted emission with a single mirror.

The upconverted emission intensities as a function of concentration are depicted in Figures 18A and 18B for the upconverting particles dispersed in water and ethanol, respectively.

In these figures, the effect of placing mirrors on different sides of the cuvette is demonstrated. As shown in these figures, the presence of mirrors leads to further enhancement of the visible upconverted emission by nearly a factor of three, for a wide range of concentrations. Figures 19A and B confirm the expected observation that the upconversion emission is more intense when ethanol is used as the dispersion medium compared to water. This can be attributed to the low absorption of 980 nm light by ethanol, as mentioned earlier.

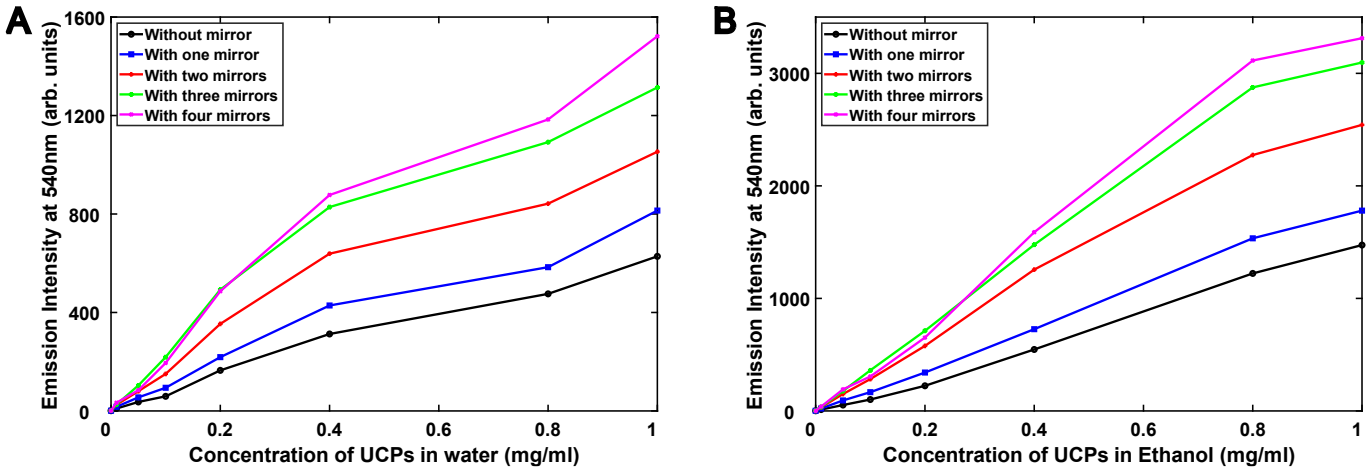

Figure 19- Effect on emission intensity at 540nm by placing one, two, three, and four mirrors on the sides of the cuvette containing UCPs dispersed in (**A**) water and (**B**) ethanol

Effect of the excitation light intensity on upconversion intensity

Figure 20 illustrates the quadratic relationship between the input light intensity at 980 nm and the output light intensity at 540 nm for different concentrations (0.25, 0.5, 1, 2 mg/mL). The quadratic nature of the curves clearly demonstrates that higher power densities lead to increased upconversion efficiencies. These data also provide a reason why it is very difficult to achieve upconverted intensities higher than three or four times, even if we place mirrors all around the cuvette. The intensity of the scattered IR light and the IR light after several reflections decreases

to an extent (power per unit area) due to the loss of the mirrors, which results in lowering two-photon upconversion luminescent. Furthermore, Figure 20 indicates that as the concentration increases, the second derivative of the curve also increases, indicating a steeper slope and higher upconversion efficiency, as expected.

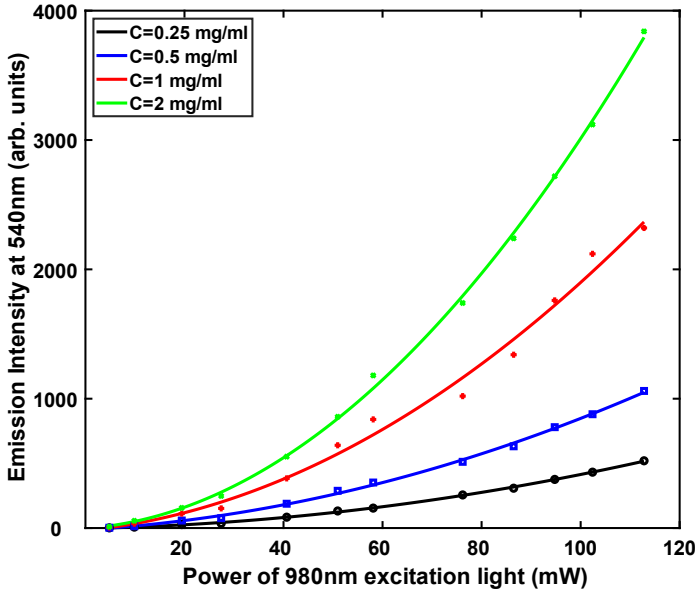

Figure 20- Effect of the concentration of upconverting particles on the slope of the power of excitation light intensity versus the upconverted emission light intensity.

Bleaching of Rhodopsin with upconverting particles

An intriguing experiment was conducted to demonstrate the conversion of infrared (IR) to visible light by examining the bleaching of bovine rhodopsin, a key molecule responsible for vision in the eyes. Rhodopsin bleaching occurs only when exposed to visible light, specifically at 540 nm, while it exhibits no absorption or bleaching at 980 nm. Rhodopsin, which facilitates low light intensity vision, exhibits maximum absorption around 540 nm and no absorption at 980 nm. When a 40-microliter solution of rhodopsin was illuminated with 980 nm, 80 mW laser light for 15 minutes, no bleaching occurred. However, when upconverting particles were introduced in

front of the rhodopsin sample and illuminated with the same intensity of 980 nm IR light, the sample was rapidly bleached within milliseconds, mimicking the effect of visible light (Figure 21). This compelling result clearly demonstrated the potential of these IR-to-visible light upconverting particles to enable infrared vision.

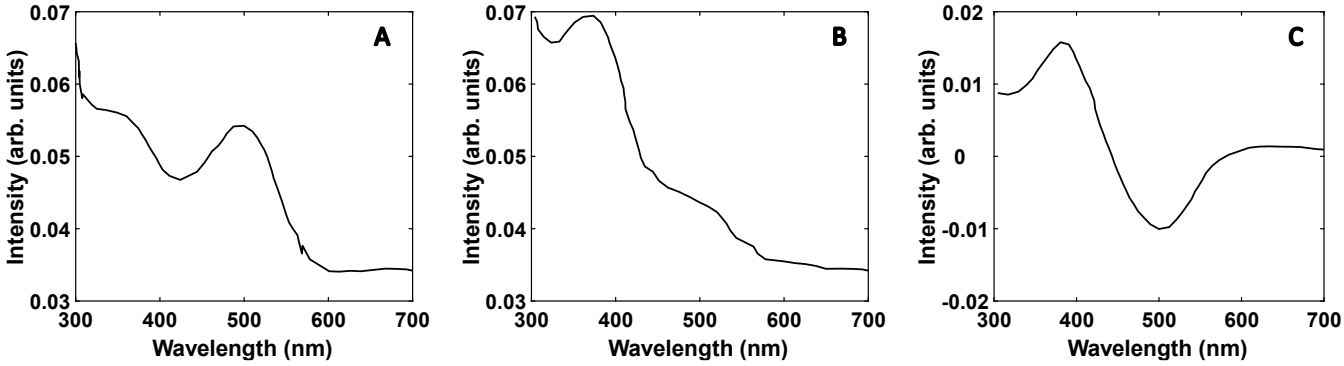

Figure 21- (**A**) Absorption spectra of rhodopsin, before bleaching and (**B**) after bleaching with 980 nm laser light in the presence of upconverting particles and (**C**) the difference absorption spectrum between before and after bleaching spectra.

Broadband, IR and visible vision glasses

We have successfully designed and fabricated optical eyeglasses that have the remarkable ability to upconvert near-infrared (NIR) light into visible green light, enabling the detection of infrared (IR) images. These glasses are coated with upconverting particles that can convert IR to visible light. The glasses incorporate a filter that selectively transmits green light while reflecting the infrared wavelengths. When an IR light image reaches the glass, it forms an image on the microparticle-coated surface. The upconverting particles convert the IR image into visible light (540 nm), which is then transmitted through the glasses for detection by the human eyes.

In Figure 22A, an example image formed on the eyeglass coated with the [NaYF4:Yb,Er] upconverting particles under 980 nm infrared illumination is displayed. The object used in the figure was the letter "A" written on a piece of glass placed in front of the coated eyeglass. The power density of the 980 nm infrared light was approximately 40 mW/cm2, while the power density of the visible light illumination was approximately 1 mW/cm2. The image shown in Figure 22A was captured by positioning a camera behind the coated eyeglass, simulating the perspective of human eyes. To ensure eye safety, a near-infrared filter is applied to the backside of the glass, protecting the eyes from intense near-infrared light. This additional filter enhances the intensity of the green image by allowing the reflected 980 nm light to pass through the upconverting particles once again.

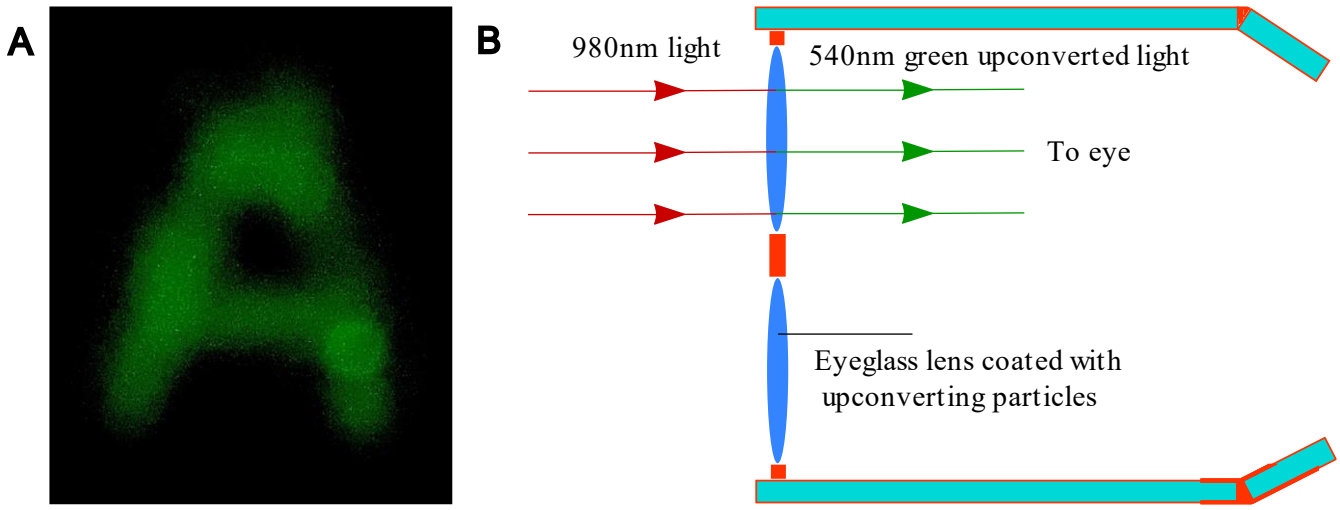

Figure 22- (**A**) Image recorded through the described optical eyeglasses under 980 nm infrared illumination and (**B**) 980 nm to vision glasses fabricated by upconverting micro-particles dispersed in clear resin.

Low-cost absorption microspectrophotometer

In this study, our objective was also to investigate and characterize the action spectrum of the living cells of Chlamydomonas reinhardtii. By conducting this analysis, we aimed to gain

valuable insights into the light-capturing properties and photosynthetic processes occurring within these cells. To measure the action spectrum of the living cells, a common approach is to use spectroscopy techniques such as microphotospectroscopy as we discussed before. To that effect, the selected wavelength of light (400-700 nm) is directed onto the Chlamydomonas reinhardtii cells through the microscope we discussed in method section. Then, the transmitted light is collected, and its intensity at every wavelength is measured using the spectrometer. The measured intensities at different wavelengths are used to construct the action spectrum of the Chlamydomonas reinhardtii living cells as shown in Figure 23. This absorption is essentially due to the chlorophylls and the carotenoids. This spectrum represents the efficiency of light absorption by these cells at different wavelengths and provides insights into the pigment's light-harvesting capabilities. Figure 24 displays an image depicting a single cell of Chlamydomonas reinhardtii under the microscope with 100X magnification.

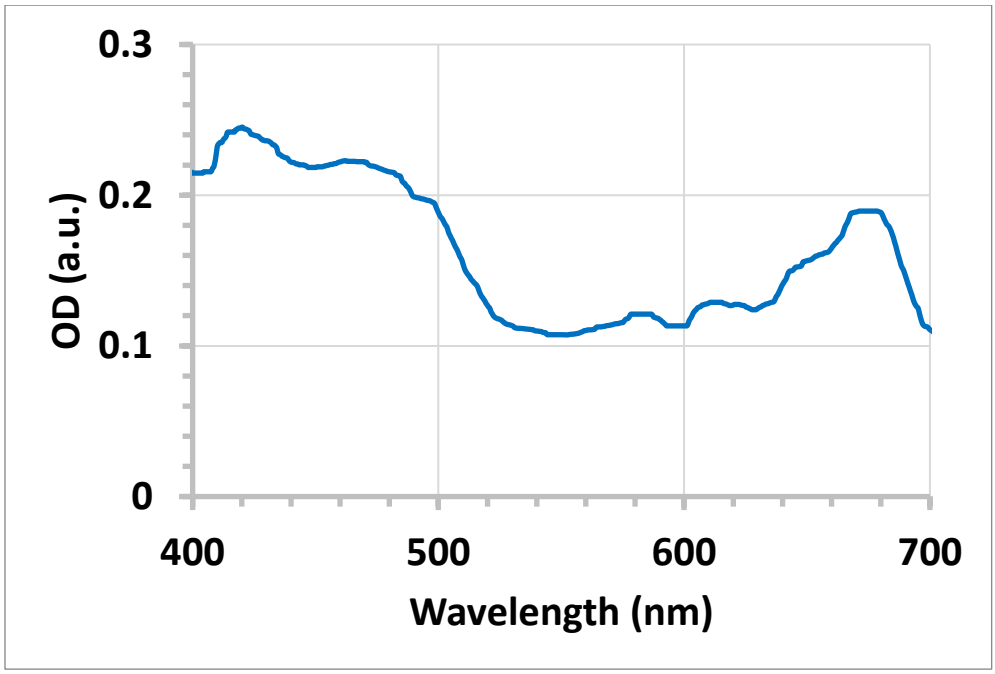

Figure 23- Steady-state absorption spectrum of Chlamydomonas reinhardtii recorded using our homebuilt visible light microscope.

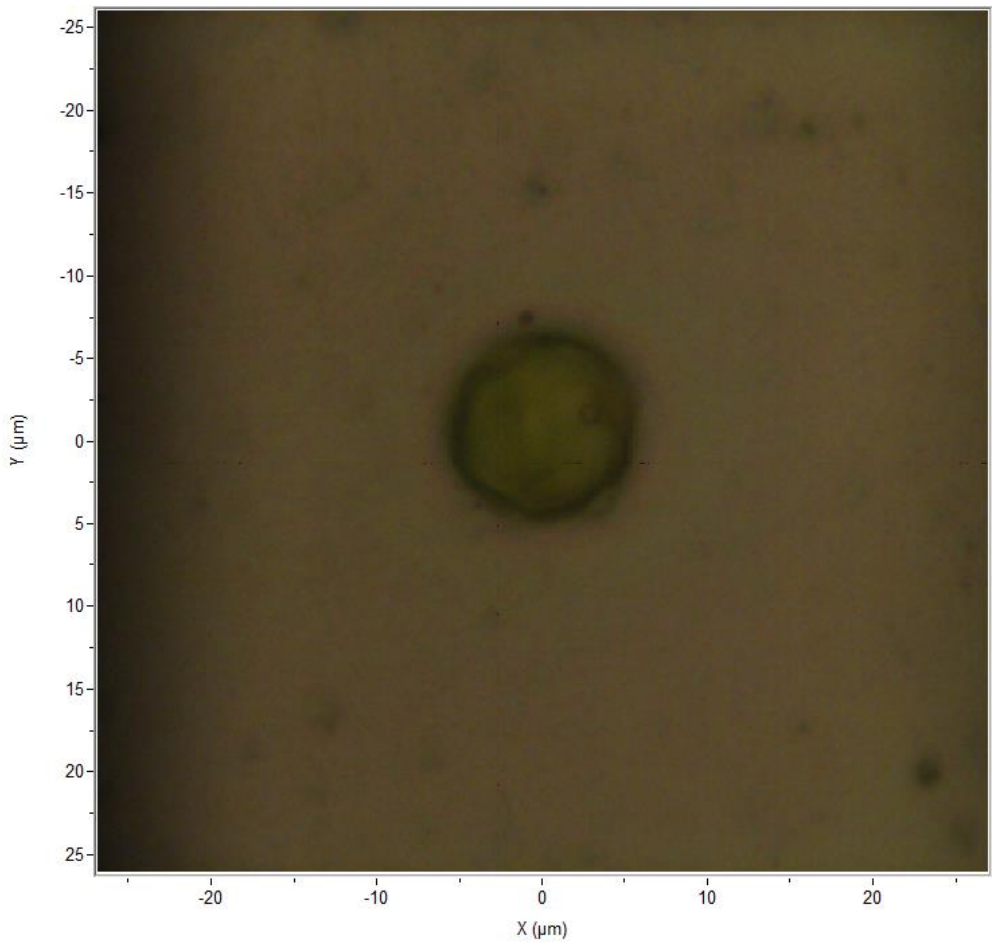

Figure 24- Microscopic Images of the Chlamydomonas reinhardtii single Cell.

By utilizing a 638 nm LED light as an excitation source, we also successfully obtained the emission spectrum of Chlamydomonas reinhardtii cells. The results, showcased in Figure 25, reveal a pronounced peak at 685 nm, highlighting the dominant emission wavelength.

By employing this well-designed experimental setup, combining the power of microscopy and spectroscopy, our study was able to investigate the absorption spectrum of Chlamydomonas reinhardtii cells with enhanced precision and accuracy. The utilization of these advanced techniques and equipment contributes to the reliability and quality of the data obtained, thereby strengthening the scientific rigor of our research.

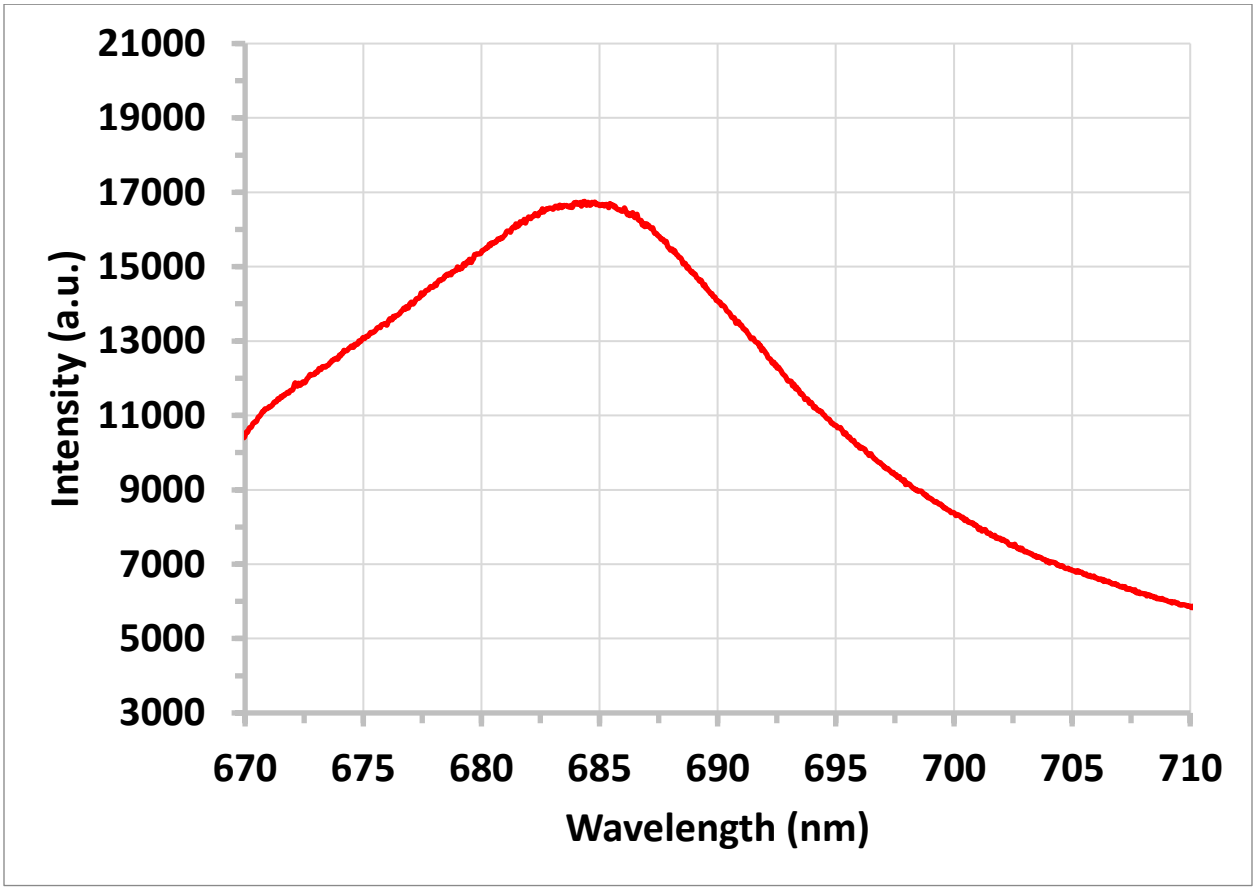

Figure 25- Emission spectrum (excitation at 638nm) of Chlamydomonas reinhardtii recorded using our homebuilt visible light Microscope.

CHAPTER IV

CONCLUSIONS AND OUTLOOK

We have studied the process of IR to visible light upconversion using rare-earth ion doped micro-particles ($NaYF_4$:Yb,Er), which are one of the most efficient sensitizers and activator materials used for up-converting infrared light to visible. In particular, we studied the two-photon stepwise nonlinear process for the conversion of 980 nm IR excitation light to 540 nm visible light. The increase in the intensity of the upconverted green light was studied, also as a function of microparticle concentration and by the placement of reflective mirrors on the sides of the cell that contain the microparticles. This made it possible to increase the intensity of the upconverted 540 nm light several times. In addition, the use of ethanol instead of water as the solvent increased the intensity of 540 nm light significantly.

We, also, were able to utilize upconverting particles to bleach rhodopsin, which is responsible for vision, using 980 nm infrared light, interacting with upconverting particles, which shows that these particles can be used to induce vision in the infrared region. In addition, we designed and constructed thin eyeglass lenses that are coated with the UCPs and can be used to convert NIR images to 540 nm visible light images. We are now studying various nano and micron-sized materials and methods in order to increase severalfold the IR to visible upconversion efficiency.

Additionally, we describe the design, construction and utilization of cost-effective microscopetrophotometer instruments that have facilitated the accurate recording of absorption and emission spectra for microscopic samples. These instruments have been designed using

readily accessible and affordable components, offering a versatile solution with broad potential applications. They enable investigations spanning biomolecular spectra analysis, identification, and quantitation of biological species and molecules at low volumes and concentrations, as well as the examination of protein crystals, biological cells, molecules, and inorganic samples on a micron scale. The affordability and accessibility of this instrument make it a valuable tool for researchers seeking to explore and analyze a wide range of microscopic samples across various scientific domains.

REFERENCES

[1] S. Wilhelm *et al.*, "Water dispersible upconverting nanoparticles: effects of surface modification on their luminescence and colloidal stability," *Nanoscale*, vol. 7, no. 4, pp. 1403-10, Jan 28 2015, doi: 10.1039/c4nr05954a.

[2] D. Yang, J. Qiu, and G. Dong, "Special optical performance from single upconverting micro/nanoparticles," *Journal of Applied Physics*, vol. 129, no. 21, 2021, doi: 10.1063/5.0052876.

[3] Z. Zhang *et al.*, "Enhanced upconversion luminescence and temperature sensing performance in Er3+/Yb3+ -codoped K3ScF6 phosphors induced by tridoping with Bi3+ ions," *Journal of Alloys and Compounds*, vol. 930, 2023, doi: 10.1016/j.jallcom.2022.167357.

[4] N. Bloembergen, "Solid State Infrared Quantum Counters," *Physical Review Letters*, vol. 2, no. 3, pp. 84-85, 02/01/ 1959, doi: 10.1103/PhysRevLett.2.84.

[5] F. Auzel, "Upconversion and Anti-Stokes Processes with f and d Ions in Solids," *Chemical Reviews*, vol. 104, no. 1, pp. 139-174, 2004/01/01 2004, doi: 10.1021/cr020357g.

[6] Y. Liu *et al.*, "Amplified stimulated emission in upconversion nanoparticles for super-resolution nanoscopy," *Nature*, vol. 543, no. 7644, pp. 229-233, Mar 9 2017, doi: 10.1038/nature21366.

[7] E. Y. Chen, C. Milleville, J. M. O. Zide, M. F. Doty, and J. Zhang, "Upconversion of low-energy photons in semiconductor nanostructures for solar energy harvesting," *MRS Energy & Sustainability*, vol. 5, no. 1, 2018, doi: 10.1557/mre.2018.15.

[8] A. Khare, "A critical review on the efficiency improvement of upconversion assisted solar cells," *Journal of Alloys and Compounds,* vol. 821, 2020, doi: 10.1016/j.jallcom.2019.153214.

[9] Y. Shang, S. Hao, C. Yang, and G. Chen, "Enhancing Solar Cell Efficiency Using Photon Upconversion Materials," *Nanomaterials (Basel),* vol. 5, no. 4, pp. 1782-1809, Oct 27 2015, doi: 10.3390/nano5041782.

[10] A. Baride, G. Sigdel, W. M. Cross, J. J. Kellar, and P. S. May, "Near Infrared-to-Near Infrared Upconversion Nanocrystals for Latent Fingerprint Development," *ACS Applied Nano Materials,* vol. 2, no. 7, pp. 4518-4527, 2019, doi: 10.1021/acsanm.9b00890.

[11] M. Wang *et al.*, "NIR-induced highly sensitive detection of latent finger-marks by NaYF(4):Yb,Er upconversion nanoparticles in a dry powder state," *Nano Res,* vol. 8, no. 6, pp. 1800-1810, Jun 2015, doi: 10.1007/s12274-014-0686-6.

[12] K. Malhotra *et al.*, "Lanthanide-Doped Upconversion Nanoparticles: Exploring A Treasure Trove of NIR-Mediated Emerging Applications," *ACS Appl Mater Interfaces,* Jan 5 2023, doi: 10.1021/acsami.2c12370.

[13] M. Patel, M. Meenu, J. K. Pandey, P. Kumar, and R. Patel, "Recent development in upconversion nanoparticles and their application in optogenetics: A review," *Journal of Rare Earths,* vol. 40, no. 6, pp. 847-861, 2022, doi: 10.1016/j.jre.2021.10.003.

[14] J. Yan, C. Li, and J. Liu, "Remotely Ameliorating Blood Glucose Levels in Type 2 Diabetes Via a Near-Infrared Laser," *Advanced Functional Materials,* vol. 31, no. 8, 2020, doi: 10.1002/adfm.202007215.

[15] L. Cheng, C. Wang, and Z. Liu, "Upconversion nanoparticles and their composite nanostructures for biomedical imaging and cancer therapy," *Nanoscale,* vol. 5, no. 1, pp. 23-37, Jan 7 2013, doi: 10.1039/c2nr32311g.

[16] M. Nyk, R. Kumar, T. Y. Ohulchanskyy, E. J. Bergey, and P. N. Prasad, "High Contrast in Vitro and in Vivo Photoluminescence Bioimaging Using Near Infrared to Near Infrared Up-Conversion in Tm3+ and Yb3+ Doped Fluoride Nanophosphors," *Nano Letters,* vol. 8, no. 11, pp. 3834-3838, 2008/11/12 2008, doi: 10.1021/nl802223f.

[17] Q.-C. Sun, Y. C. Ding, D. M. Sagar, and P. Nagpal, "Photon upconversion towards applications in energy conversion and bioimaging," *Progress in Surface Science,* vol. 92, no. 4, pp. 281-316, 2017, doi: 10.1016/j.progsurf.2017.09.003.

[18] A. Gomes, M. Neves, and J. A. S. Cavaleiro, "Cancer, Photodynamic Therapy and Porphyrin-Type Derivatives," *An Acad Bras Cienc,* vol. 90, no. 1 Suppl 2, pp. 993-1026, 2018, doi: 10.1590/0001-3765201820170811.

[19] N. M. Idris, M. K. Gnanasammandhan, J. Zhang, P. C. Ho, R. Mahendran, and Y. Zhang, "In vivo photodynamic therapy using upconversion nanoparticles as remote-controlled nanotransducers," *Nat Med,* vol. 18, no. 10, pp. 1580-5, Oct 2012, doi: 10.1038/nm.2933.

[20] S. Hao, G. Chen, and C. Yang, "Sensing using rare-earth-doped upconversion nanoparticles," *Theranostics,* vol. 3, no. 5, pp. 331-45, 2013, doi: 10.7150/thno.5305.

[21] C. A. Tajon *et al.*, "Photostable and efficient upconverting nanocrystal-based chemical sensors," *Opt Mater (Amst),* vol. 84, pp. 345-353, Oct 2018, doi: 10.1016/j.optmat.2018.07.031.

[22] S. Wilhelm, "Perspectives for Upconverting Nanoparticles," *ACS Nano,* vol. 11, no. 11, pp. 10644-10653, Nov 28 2017, doi: 10.1021/acsnano.7b07120.

[23] Y. Zhang, "Topical Collection “Upconversion fluorescent nanomaterials for biodetection and bioimaging”," *Microchimica Acta,* vol. 190, no. 1, p. 23, 2022/12/14 2022, doi: 10.1007/s00604-022-05606-w.

[24] B. Gu and Q. Zhang, "Recent Advances on Functionalized Upconversion Nanoparticles for Detection of Small Molecules and Ions in Biosystems," *Adv Sci (Weinh),* vol. 5, no. 3, p. 1700609, Mar 2018, doi: 10.1002/advs.201700609.

[25] F. Wang and X. Liu, "Recent advances in the chemistry of lanthanide-doped upconversion nanocrystals," *Chem Soc Rev,* vol. 38, no. 4, pp. 976-89, Apr 2009, doi: 10.1039/b809132n.

[26] X. Zhu, J. Zhang, J. Liu, and Y. Zhang, "Recent Progress of Rare-Earth Doped Upconversion Nanoparticles: Synthesis, Optimization, and Applications," *Adv Sci (Weinh),* vol. 6, no. 22, p. 1901358, Nov 2019, doi: 10.1002/advs.201901358.

[27] D. J. Gargas *et al.*, "Engineering bright sub-10-nm upconverting nanocrystals for single-molecule imaging," *Nat Nanotechnol,* vol. 9, no. 4, pp. 300-5, Apr 2014, doi: 10.1038/nnano.2014.29.

[28] A. Gnach, T. Lipinski, A. Bednarkiewicz, J. Rybka, and J. A. Capobianco, "Upconverting nanoparticles: assessing the toxicity," *Chemical Society Reviews,* 10.1039/C4CS00177J vol. 44, no. 6, pp. 1561-1584, 2015, doi: 10.1039/C4CS00177J.

[29] X. Cheng *et al.*, "Recent Development in Sensitizers for Lanthanide-Doped Upconversion Luminescence," *Chem Rev,* vol. 122, no. 21, pp. 15998-16050, Nov 9 2022, doi: 10.1021/acs.chemrev.1c00772.

[30] C. Ma, C. Shan, K. Park, A. T. Mok, P. J. Antonick, and X. Yang, "Enhancing the generating and collecting efficiency of single particle upconverting luminescence at low

power excitation," *Nanophotonics*, vol. 9, no. 7, pp. 1993-2000, 2020, doi: 10.1515/nanoph-2019-0526.

[31] K. Zajdel, J. Janowska, M. Frontczak-Baniewicz, J. Sypecka, and B. Sikora, "Upconverting Nanoparticles as a New Bio-Imaging Strategy—Investigating Intracellular Trafficking of Endogenous Processes in Neural Tissue," *International Journal of Molecular Sciences*, vol. 24, no. 2, 2023, doi: 10.3390/ijms24021122.

[32] Y. Chen *et al.*, "NaYF4 upconversion crystals with red light emission by low Er3+ concentration doping," *Optik*, vol. 272, p. 170287, 2023/02/01/ 2023, doi: https://doi.org/10.1016/j.ijleo.2022.170287.

[33] F. Fanjul-Vélez and J. L. Arce-Diego, "Light propagation in turbid media: Application to biological tissues," in *Proceedings of 21st International Conference Radioelektronika 2011*, 19-20 April 2011 2011, pp. 1-4, doi: 10.1109/RADIOELEK.2011.5936483.

[34] Y. Pu, J. Chen, W. Wang, and R. R. Alfano, "Basic Optical Scattering Parameter of the Brain and Prostate Tissues in the Spectral Range of 400–2400 nm," in *Neurophotonics and Biomedical Spectroscopy*, 2019, pp. 229-252.

[35] S. Han, R. Deng, X. Xie, and X. Liu, "Enhancing luminescence in lanthanide-doped upconversion nanoparticles," *Angew Chem Int Ed Engl*, vol. 53, no. 44, pp. 11702-15, Oct 27 2014, doi: 10.1002/anie.201403408.

[36] X. Liu, C. H. Yan, and J. A. Capobianco, "Photon upconversion nanomaterials," *Chem Soc Rev*, vol. 44, no. 6, pp. 1299-301, Mar 21 2015, doi: 10.1039/c5cs90009c.

[37] J. Galego, F. J. Garcia-Vidal, and J. Feist, "Many-Molecule Reaction Triggered by a Single Photon in Polaritonic Chemistry," *Phys Rev Lett*, vol. 119, no. 13, p. 136001, Sep 29 2017, doi: 10.1103/PhysRevLett.119.136001.

[38] Y. Kobayashi and J. Abe, "Recent advances in low-power-threshold nonlinear photochromic materials," *Chem Soc Rev,* vol. 51, no. 7, pp. 2397-2415, Apr 4 2022, doi: 10.1039/d1cs01144h.

[39] B. A. Lengyel, "Lasers: generation of light by stimulated emission," 1962.

[40] L. Galas *et al.*, "“Probe, Sample, and Instrument (PSI)”: The Hat-Trick for Fluorescence Live Cell Imaging," *Chemosensors,* vol. 6, no. 3, 2018, doi: 10.3390/chemosensors6030040.

[41] M. Rumi and J. W. Perry, "Two-photon absorption: an overview of measurements and principles," *Advances in Optics and Photonics,* vol. 2, no. 4, 2010, doi: 10.1364/aop.2.000451.

[42] M. Göppert-Mayer, "Elementary processes with two quantum transitions," *Annalen der Physik,* vol. 18, no. 7-8, pp. 466-479, 2009.

[43] B. E. A. Saleh, B. M. Jost, H.-B. Fei, and M. C. Teich, "Entangled-Photon Virtual-State Spectroscopy," *Physical Review Letters,* vol. 80, no. 16, pp. 3483-3486, 04/20/ 1998, doi: 10.1103/PhysRevLett.80.3483.

[44] Y. Kobayashi, K. Mutoh, and J. Abe, "Stepwise two-photon absorption processes utilizing photochromic reactions," *Journal of Photochemistry and Photobiology C: Photochemistry Reviews,* vol. 34, pp. 2-28, 2018, doi: 10.1016/j.jphotochemrev.2017.12.006.

[45] M. Pawlicki, H. A. Collins, R. G. Denning, and H. L. Anderson, "Two-photon absorption and the design of two-photon dyes," *Angew Chem Int Ed Engl,* vol. 48, no. 18, pp. 3244-66, 2009, doi: 10.1002/anie.200805257.

[46] W. Kaiser and C. G. B. Garrett, "Two-Photon Excitation in CaF2:Eu2+," *Physical Review Letters,* vol. 7, no. 6, pp. 229-231, 1961, doi: 10.1103/PhysRevLett.7.229.

[47] J. Feng, J. Alves, D. M. de Clercq, and T. W. Schmidt, "Photochemical Upconversion," *Annu Rev Phys Chem,* vol. 74, pp. 145-168, Apr 24 2023, doi: 10.1146/annurev-physchem-092722-104952.

[48] G. Chen, H. Qiu, P. N. Prasad, and X. Chen, "Upconversion nanoparticles: design, nanochemistry, and applications in theranostics," *Chem Rev,* vol. 114, no. 10, pp. 5161-214, May 28 2014, doi: 10.1021/cr400425h.

[49] G. Chen, G. Somesfalean, Y. Liu, Z. Zhang, Q. Sun, and F. Wang, "Upconversion mechanism for two-color emission in rare-earth-ion-dopedZrO2nanocrystals," *Physical Review B,* vol. 75, no. 19, 2007, doi: 10.1103/PhysRevB.75.195204.

[50] M. Manoj Kumar, H. Hans Christian, and V. Ulrich, "Photon-Upconverting Materials: Advances and Prospects for Various Emerging Applications," in *Luminescence,* T. Jagannathan Ed. Rijeka: IntechOpen, 2016, p. Ch. 6.

[51] G. Liang *et al.*, "Recent progress in the development of upconversion nanomaterials in bioimaging and disease treatment," *J Nanobiotechnology,* vol. 18, no. 1, p. 154, Oct 29 2020, doi: 10.1186/s12951-020-00713-3.

[52] R. Martín-Rodríguez, F. T. Rabouw, M. Trevisani, M. Bettinelli, and A. Meijerink, "Upconversion Dynamics in Er3+-Doped Gd2O2S: Influence of Excitation Power, Er3+Concentration, and Defects," *Advanced Optical Materials,* vol. 3, no. 4, pp. 558-567, 2015, doi: 10.1002/adom.201400588.

[53] K. L. Reddy, N. Prabhakar, R. Arppe, J. M. Rosenholm, and V. Krishnan, "Microwave-assisted one-step synthesis of acetate-capped NaYF4:Yb/Er upconversion nanocrystals

and their application in bioimaging," *Journal of Materials Science,* vol. 52, no. 10, pp. 5738-5750, 2017, doi: 10.1007/s10853-017-0809-z.

[54] L. D. Sun, H. Dong, P. Z. Zhang, and C. H. Yan, "Upconversion of rare Earth nanomaterials," *Annu Rev Phys Chem,* vol. 66, pp. 619-42, Apr 2015, doi: 10.1146/annurev-physchem-040214-121344.

[55] H. Liang, G. Chen, L. Li, Y. Liu, F. Qin, and Z. Zhang, "Upconversion luminescence in Yb3+/Tb3+-codoped monodisperse NaYF4 nanocrystals," *Optics Communications,* vol. 282, no. 14, pp. 3028-3031, 2009, doi: 10.1016/j.optcom.2009.04.006.

[56] Y. Dwivedi, S. N. Thakur, and S. B. Rai, "Study of frequency upconversion in Yb3+/Eu3+ by cooperative energy transfer in oxyfluoroborate glass matrix," *Applied Physics B,* vol. 89, no. 1, pp. 45-51, 2007, doi: 10.1007/s00340-007-2747-y.

[57] A. A. Pushkar', T. V. Uvarova, and V. V. Kiiko, "Up-conversion multiwave (White) luminescence in the visible spectral range under excitation by IR laser diodes in the active BaY2F8:Yb3+,Pr3+ medium," *Optics and Spectroscopy,* vol. 111, no. 2, pp. 273-276, 2011, doi: 10.1134/s0030400x1108025x.

[58] M. Haase and H. Schafer, "Upconverting nanoparticles," *Angew Chem Int Ed Engl,* vol. 50, no. 26, pp. 5808-29, Jun 20 2011, doi: 10.1002/anie.201005159.

[59] F. Wang and X. Liu, "Recent advances in the chemistry of lanthanide-doped upconversion nanocrystals," *Chemical Society Reviews,* vol. 38, no. 4, p. 976, 2009-01-01 2009, doi: 10.1039/b809132n.

[60] O. S. Wenger and H. U. Güdel, "Chemical Tuning of the Photon Upconversion Properties in Ti²⁺-Doped Chloride Host Lattices," *Inorganic Chemistry,* vol. 40, no. 23, pp. 5747-5753, 2001, doi: 10.1021/ic010255t.

[61] O. S. Wenger, S. Bénard, and H. U. Güdel, "Crystal Field Effects on the Optical Absorption and Luminescence Properties of Ni2+-Doped Chlorides and Bromides: Crossover in the Emitting Higher Excited State," *Inorganic Chemistry*, vol. 41, no. 23, pp. 5968-5977, 2002/11/01 2002, doi: 10.1021/ic020347y.

[62] D. R. Gamelin and H. U. Güdel, "Spectroscopy and Dynamics of Re4+ Near-IR-to-Visible Luminescence Upconversion," *Inorganic Chemistry*, vol. 38, no. 22, pp. 5154-5164, 1999/11/01 1999, doi: 10.1021/ic990556r.

[63] W. Markus and U. G. Hans, "Luminescence spectroscopy and NIR to VIS upconversion of Cs2GeF6: 2% Re4+," *Journal of Physics: Condensed Matter*, vol. 13, no. 42, p. 9583, 2001/10/05 2001, doi: 10.1088/0953-8984/13/42/317.

[64] M. Wermuth and H. U. Güdel, "Photon avalanche in Cs2ZrCl6: Os4+," *The Journal of Chemical Physics*, vol. 114, no. 3, pp. 1393-1404, 2001, doi: 10.1063/1.1334350.

[65] P. J. Dereń, W. Stręk, E. Zych, and J. Drożdżyński, "Up-conversion in elpasolite crystals doped with U3+," *Chemical Physics Letters*, vol. 332, no. 3, pp. 308-312, 2000/12/22/ 2000, doi: https://doi.org/10.1016/S0009-2614(00)01249-5.

[66] F. Huang, X. Liu, Y. Ma, S. Kang, L. Hu, and D. Chen, "Origin of near to middle infrared luminescence and energy transfer process of Er(3+)/Yb(3+)co-doped fluorotellurite glasses under different excitations," *Sci Rep*, vol. 5, p. 8233, Feb 4 2015, doi: 10.1038/srep08233.

[67] R. K. Watts and H. J. Richter, "Diffusion and Transfer of Optical Excitation in YF3: Yb, Ho," *Physical Review B*, vol. 6, no. 4, pp. 1584-1589, 1972, doi: 10.1103/physrevb.6.1584.

[68] B. Jacquier, C. Linare`s, R. Mahiou, J. L. Adam, E. De´noue, and J. Lucas, "Efficient blue upconversion in Tm3+ and Pr3+ doped BIGaZYbTZr glasses," *Journal of Luminescence,* vol. 60-61, pp. 175-178, 1994/04/01/ 1994, doi: https://doi.org/10.1016/0022-2313(94)90123-6.

[69] H. Schäfer, P. Ptacek, K. Kömpe, and M. Haase, "Lanthanide-Doped NaYF4 Nanocrystals in Aqueous Solution Displaying Strong Up-Conversion Emission," *Chemistry of Materials,* vol. 19, no. 6, pp. 1396-1400, 2007/03/01 2007, doi: 10.1021/cm062385b.

[70] P. R. Diamente, M. Raudsepp, and F. C. J. M. van Veggel, "Dispersible Tm3+-Doped Nanoparticles that Exhibit Strong 1.47 μm Photoluminescence," *Advanced Functional Materials,* https://doi.org/10.1002/adfm.200600142 vol. 17, no. 3, pp. 363-368, 2007/02/12 2007, doi: https://doi.org/10.1002/adfm.200600142.

[71] R. A. Hewes and J. F. Sarver, "Infrared Excitation Processes for the Visible Luminescence of ${\mathrm{Er}}^{3+}$, ${\mathrm{Ho}}^{3+}$, and ${\mathrm{Tm}}^{3+}$ in ${\mathrm{Yb}}^{3+}$-Sensitized Rare-Earth Trifluorides," *Physical Review,* vol. 182, no. 2, pp. 427-436, 06/10/ 1969, doi: 10.1103/PhysRev.182.427.

[72] N. J. Cockroft, G. D. Jones, and D. C. Nguyen, "Dynamics and spectroscopy of infrared-to-visible upconversion in erbium-doped cesium cadmium bromide (${\mathrm{CsCdBr}}_{3}$:${\mathrm{Er}}^{3+}$)," *Physical Review B,* vol. 45, no. 10, pp. 5187-5198, 03/01/ 1992, doi: 10.1103/PhysRevB.45.5187.

[73] J. F. Suyver, J. Grimm, M. K. van Veen, D. Biner, K. W. Krämer, and H. U. Güdel, "Upconversion spectroscopy and properties of NaYF4 doped with Er3+, Tm3+ and/or

Yb3+," *Journal of Luminescence*, vol. 117, no. 1, pp. 1-12, 2006/03/01/ 2006, doi: https://doi.org/10.1016/j.jlumin.2005.03.011.

[74] N. Menyuk, K. Dwight, and J. W. Pierce, "NaYF4 : Yb,Er—an efficient upconversion phosphor," *Applied Physics Letters*, vol. 21, no. 4, pp. 159-161, 2003, doi: 10.1063/1.1654325.

[75] G. Blasse and B. C. Grabmaier, "A General Introduction to Luminescent Materials," in *Luminescent Materials*, G. Blasse and B. C. Grabmaier Eds. Berlin, Heidelberg: Springer Berlin Heidelberg, 1994, pp. 1-9.

[76] C. M. S. Calado *et al.*, "Defect disorder and optical spectroscopy study of Eu-doped NaYF₄ and NaYGdF₄ nanoparticles," *Optical Materials*, vol. 137, p. 113529, March 01, 2023 2023, doi: 10.1016/j.optmat.2023.113529.

[77] R. E. Thoma, G. M. Hebert, H. Insley, and C. F. Weaver, "Phase Equilibria in the System Sodium Fluoride-Yttrium Fluoride," *Inorganic Chemistry*, vol. 2, no. 5, pp. 1005-1012, 1963/10/01 1963, doi: 10.1021/ic50009a030.

[78] H.-X. Mai *et al.*, "High-Quality Sodium Rare-Earth Fluoride Nanocrystals: Controlled Synthesis and Optical Properties," *Journal of the American Chemical Society*, vol. 128, no. 19, pp. 6426-6436, 2006/05/01 2006, doi: 10.1021/ja060212h.

[79] R. Kumar, M. Nyk, T. Y. Ohulchanskyy, C. A. Flask, and P. N. Prasad, "Combined Optical and MR Bioimaging Using Rare Earth Ion Doped NaYF4 Nanocrystals," *Advanced Functional Materials*, https://doi.org/10.1002/adfm.200800765 vol. 19, no. 6, pp. 853-859, 2009/03/24 2009, doi: https://doi.org/10.1002/adfm.200800765.

[80] K. W. Krämer, D. Biner, G. Frei, H. U. Güdel, M. P. Hehlen, and S. R. Lüthi, "Hexagonal Sodium Yttrium Fluoride Based Green and Blue Emitting Upconversion

Phosphors," *Chemistry of Materials*, vol. 16, no. 7, pp. 1244-1251, 2004/04/01 2004, doi: 10.1021/cm031124o.

[81] M. Kaiser, C. Würth, M. Kraft, I. Hyppänen, T. Soukka, and U. Resch-Genger, "Power-dependent upconversion quantum yield of NaYF4:Yb3+,Er3+ nano- and micrometer-sized particles – measurements and simulations," *Nanoscale*, 10.1039/C7NR02449E vol. 9, no. 28, pp. 10051-10058, 2017, doi: 10.1039/C7NR02449E.

[82] R. H. Page *et al.*, "Upconversion-pumped luminescence efficiency of rare-earth-doped hosts sensitized with trivalent ytterbium," *J. Opt. Soc. Am. B*, vol. 15, no. 3, pp. 996-1008, 1998/03/01 1998, doi: 10.1364/JOSAB.15.000996.

[83] Y. Hou *et al.*, "Homogenization of Optical Field in Nanocrystal-Embedded Perovskite Composites," *ACS Energy Letters*, vol. 7, no. 5, pp. 1657-1671, 2022, doi: 10.1021/acsenergylett.2c00608.

[84] T. Schulze, K. Lips, and T. W. Schmidt, "Enhancing solar cells with photochemical upconversion," *SPIE Newsroom*, 2014, doi: 10.1117/2.1201403.005390.

[85] D. W. Felsher, "Cancer revoked: oncogenes as therapeutic targets," *Nat Rev Cancer*, vol. 3, no. 5, pp. 375-80, May 2003, doi: 10.1038/nrc1070.

[86] K. Kalka, H. Merk, and H. Mukhtar, "Photodynamic therapy in dermatology," *Journal of the American Academy of Dermatology*, vol. 42, no. 3, pp. 389-413, 2000/03/01/ 2000, doi: https://doi.org/10.1016/S0190-9622(00)90209-3.

[87] M. Megna, G. Fabbrocini, C. Marasca, and G. Monfrecola, "Photodynamic Therapy and Skin Appendage Disorders: A Review," *Skin Appendage Disord*, vol. 2, no. 3-4, pp. 166-176, Jan 2017, doi: 10.1159/000453273.

[88] S. Kwiatkowski *et al.*, "Photodynamic therapy - mechanisms, photosensitizers and combinations," *Biomed Pharmacother,* vol. 106, pp. 1098-1107, Oct 2018, doi: 10.1016/j.biopha.2018.07.049.

[89] R. Saini and C. F. Poh, "Photodynamic therapy: a review and its prospective role in the management of oral potentially malignant disorders," *Oral Dis,* vol. 19, no. 5, pp. 440-51, Jul 2013, doi: 10.1111/odi.12003.

[90] C. Donohoe, M. O. Senge, L. G. Arnaut, and L. C. Gomes-da-Silva, "Cell death in photodynamic therapy: From oxidative stress to anti-tumor immunity," *Biochim Biophys Acta Rev Cancer,* vol. 1872, no. 2, p. 188308, Dec 2019, doi: 10.1016/j.bbcan.2019.07.003.

[91] K. Li *et al.*, "Advances in the application of upconversion nanoparticles for detecting and treating cancers," *Photodiagnosis Photodyn Ther,* vol. 25, pp. 177-192, Mar 2019, doi: 10.1016/j.pdpdt.2018.12.007.

[92] D. K. Chatterjee and Z. Yong, "Upconverting nanoparticles as nanotransducers for photodynamic therapy in cancer cells," *Nanomedicine,* vol. 3, no. 1, pp. 73-82, 2008/02/01 2008, doi: 10.2217/17435889.3.1.73.

[93] X. Zhang *et al.*, "Energy Pumping by Surface Collectors on Upconversion Nanoparticles for Extended Transfer and Efficient Self-Evaluable Photodynamic Therapy," *CCS Chemistry,* vol. 4, no. 4, pp. 1251-1262, 2022, doi: 10.31635/ccschem.021.202100951.

[94] Y. Wang, P. Shen, C. Li, Y. Wang, and Z. Liu, "Upconversion fluorescence resonance energy transfer based biosensor for ultrasensitive detection of matrix metalloproteinase-2 in blood," *Anal Chem,* vol. 84, no. 3, pp. 1466-73, Feb 7 2012, doi: 10.1021/ac202627b.

[95] S. M. Saleh, R. Ali, T. Hirsch, and O. S. Wolfbeis, "Detection of biotin–avidin affinity binding by exploiting a self-referenced system composed of upconverting luminescent nanoparticles and gold nanoparticles," *Journal of Nanoparticle Research,* vol. 13, no. 10, pp. 4603-4611, 2011, doi: 10.1007/s11051-011-0424-x.

[96] L. Yao, J. Zhou, J. Liu, W. Feng, and F. Li, "Iridium-Complex-Modified Upconversion Nanophosphors for Effective LRET Detection of Cyanide Anions in Pure Water," *Advanced Functional Materials,* vol. 22, no. 13, pp. 2667-2672, 2012, doi: 10.1002/adfm.201102981.

[97] J. Liu, Y. Liu, Q. Liu, C. Li, L. Sun, and F. Li, "Iridium(III) complex-coated nanosystem for ratiometric upconversion luminescence bioimaging of cyanide anions," *J Am Chem Soc,* vol. 133, no. 39, pp. 15276-9, Oct 5 2011, doi: 10.1021/ja205907y.

[98] Q. Liu, J. Peng, L. Sun, and F. Li, "High-Efficiency Upconversion Luminescent Sensing and Bioimaging of Hg(II) by Chromophoric Ruthenium Complex-Assembled Nanophosphors," *ACS Nano,* vol. 5, no. 10, pp. 8040-8048, 2011/10/25 2011, doi: 10.1021/nn202620u.

[99] H. S. Mader and O. S. Wolfbeis, "Optical Ammonia Sensor Based on Upconverting Luminescent Nanoparticles," *Analytical Chemistry,* vol. 82, no. 12, pp. 5002-5004, 2010/06/15 2010, doi: 10.1021/ac1007283.

[100] D. E. Achatz, R. J. Meier, L. H. Fischer, and O. S. Wolfbeis, "Luminescent sensing of oxygen using a quenchable probe and upconverting nanoparticles," *Angew Chem Int Ed Engl,* vol. 50, no. 1, pp. 260-3, Jan 3 2011, doi: 10.1002/anie.201004902.

[101] Y. Li, X. Liu, X. Yang, H. Lei, Y. Zhang, and B. Li, "Enhancing Upconversion Fluorescence with a Natural Bio-microlens," *ACS Nano,* vol. 11, no. 11, pp. 10672-10680, Nov 28 2017, doi: 10.1021/acsnano.7b04420.

[102] D. Dhankhar, R. Li, A. Nagpal, J. Chen, T. C. Cesario, and P. M. Rentzepis, "Extending Human Vision to Infrared and Ultraviolet Light: A Study Using Micro-Particles and Fluorescent Molecules," *IEEE Access,* vol. 8, pp. 73890-73897, 2020, doi: 10.1109/access.2020.2988398.

[103] K. Khosh Abady, D. Dankhar, A. Krishnamoorthi, and P. M. Rentzepis, "Enhancing the upconversion efficiency of NaYF(4):Yb,Er microparticles for infrared vision applications," *Sci Rep,* vol. 13, no. 1, p. 8408, May 24 2023, doi: 10.1038/s41598-023-35164-x.